UNITED NATIONS EDUCATIONAL, SCIENTIFIC AND CULTURAL ORGANIZATION
INTERNATIONAL ATOMIC ENERGY AGENCY
INTERNATIONAL CENTRE FOR THEORETICAL PHYSICS
I.C.T.P., P.O. BOX 586, 34100 TRIESTE, ITALY, CABLE: CENTRATOM TRIESTE

H4.SMR/994-23

SPRING COLLEGES IN COMPUTATIONAL PHYSICS

19 May - 27 June 1997

AB-INITIO ELECTRONIC STRUCTURE CALCULATIONS - IV, V

S. DE GIRONCOLI
S.I.S.S.A.
International School for Advanced Studies
Trieste, ITALY

3

KOHN-SHAM Phys. Rev. 140 A1133 (1965)

Let us now qualitatively discuss the appropriateness of our procedure for various classes of electronic systems.

In atoms and molecules one can distinguish three regions: (1) A region near the atomic nucleus, where the electronic density is high and therefore, in view of case (*b*) above, we expect our procedure to be satisfactory. (2) The main "body" of the charge distribution where the electronic density $n(r)$ is relatively slowly varying, so that our approximation (2.3) for ϵ_{xc} is expected to be satisfactory as discussed in case (a) above. (3) The "surface" of atoms and the overlap regions in molecules. Here our approximation (2.3) has no validity and therefore we expect this region to be the main source of error. We do not expect an accurate description of chemical binding. In large atoms, of course, this "surface" region becomes of less importance. (The surface is more satisfactorily handled in the nonlocal method described under *B* below.)

For metals, alloys, and small-gap insulators we have, of course, no surface problem and we expect our approximation (2.3) to give a good representation of exchange and correlation effects. In large-gap insulators, however, the actual correlation energy will be considerably reduced compared to that of a homogeneous electron gas of the same density.

(b): $T_s \gg E_{xc}$

(2.3): LDA

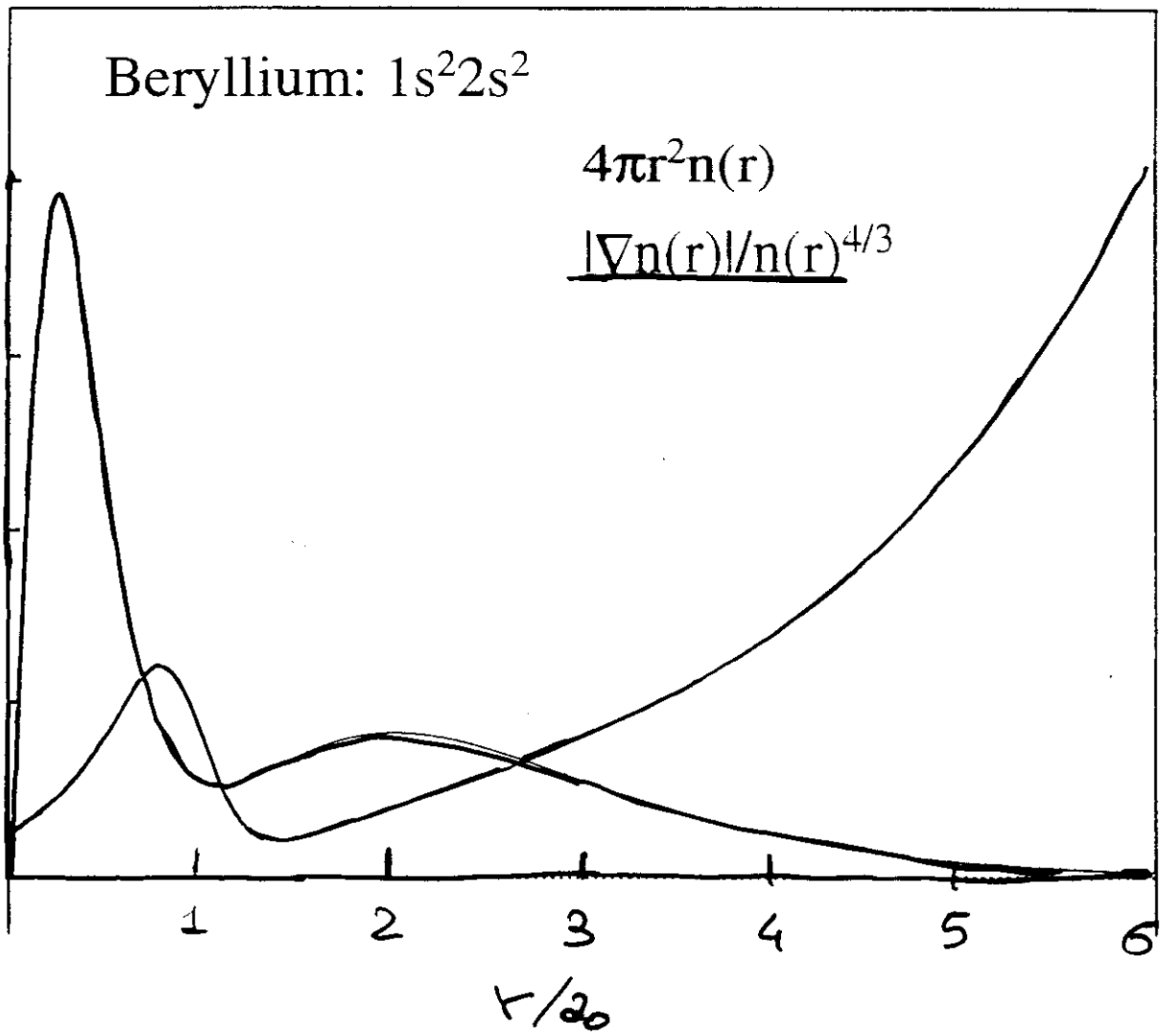
Beryllium: $1s^2 2s^2$
$4\pi r^2 n(r)$
$|\nabla n(r)|/n(r)^{4/3}$
1
2
3
4
5
6
r/a₀

Gunnarsson-Lundqvist Phys. Rev B 13, 4274 (1976)

In the first application to atoms, Tong and Sham[76] found that, while the calculated exchange energies for various atoms are about 10% too small in magnitude, the correlation energies are too large by a factor of about two, the errors partially balancing each other. The relative accuracy for both quantities improves for large atoms. The error in the exchange energy is surprisingly small, considering the nonlocal nature of the exchange forces and the strong inhomogeneity of the system. As has been pointed out by Tong,[77] the major source of error in the correlation energy is that the discreteness and the nonzero spacing of the low-lying levels of a finite system, in principle, would not be well described by expressions derived from an infinite electron liquid. A reason for the increased relative accuracy for larger atoms is the decrease of the exchange-correlation hole compared with the inhomogeneity length, as an electron shell is getting filled. All these results and arguments suggest the LSD approximation to be less satisfactory for a *detailed* description of tightly bound core electrons, while it is likely to give useful results for valence electrons. In this section we will give results supporting that view.

76 Tong and Sham, Phys. Rev. 144, 1 (1966)

77 Tong, Phys. Rev. A 4, 1375 (1971).

Total Energies of First Row Atoms

	E^{exp}	E^{HF}	E^{LSD} [Ry]
			1H = 2Ry
Li	-14.957	-14.866	-14.686
Be	-29.339	-29.150	-28.892
B	-49.318	-49.070	-48.704
C	-75.715	-75.404	-74.932
N	-109.228	-108.856	-108.256
O	-150.225	-149.716	-149.042
F	-199.618	-198.982	-198.216

E^{exp} C.W. Scherr, J.N. Silverman, F.A. Matsen, Phys. Rev. 127, 830 (1962)

E^{HF} E. Clementi, C. Roetti, At. Data Nucl. Data Tables 14 177 (1974)

E^{LSD} M.R. Norman, D.D. Koelling, Phys. Rev. B 30 5530 (1984)

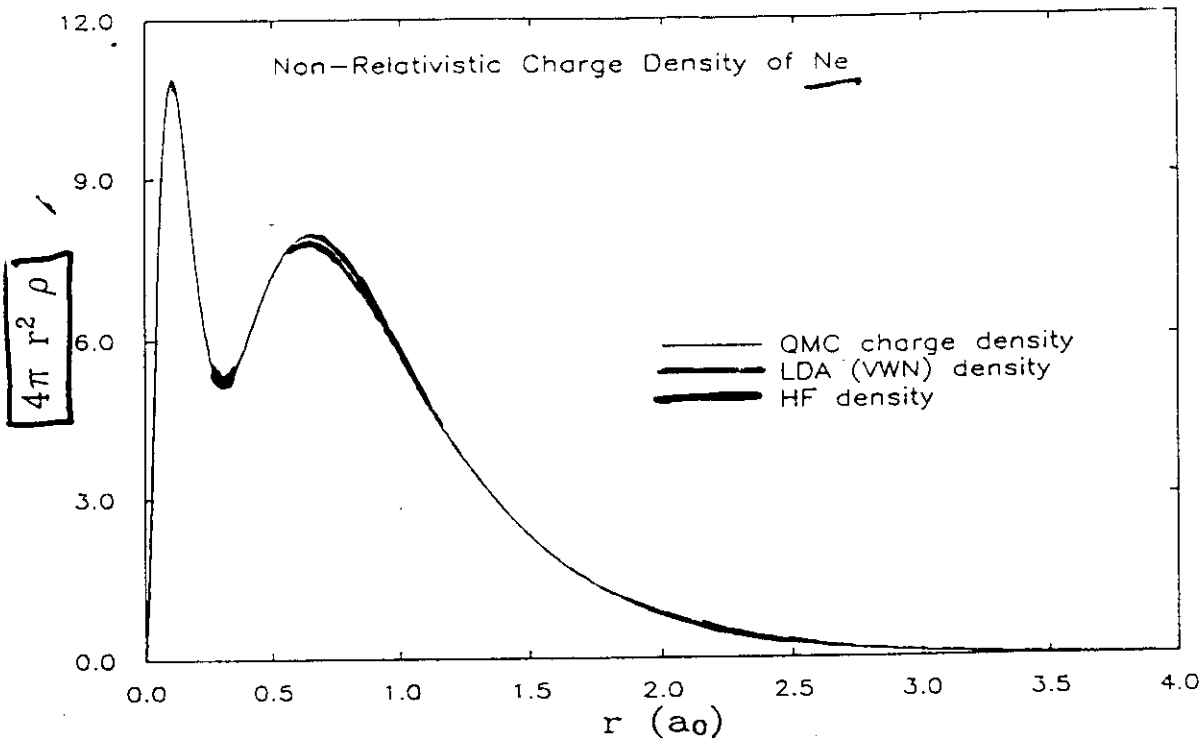

FIG. 1. Comparison of the LDA, Hartree-Fock, and quantum Monte Carlo densities for Ne.

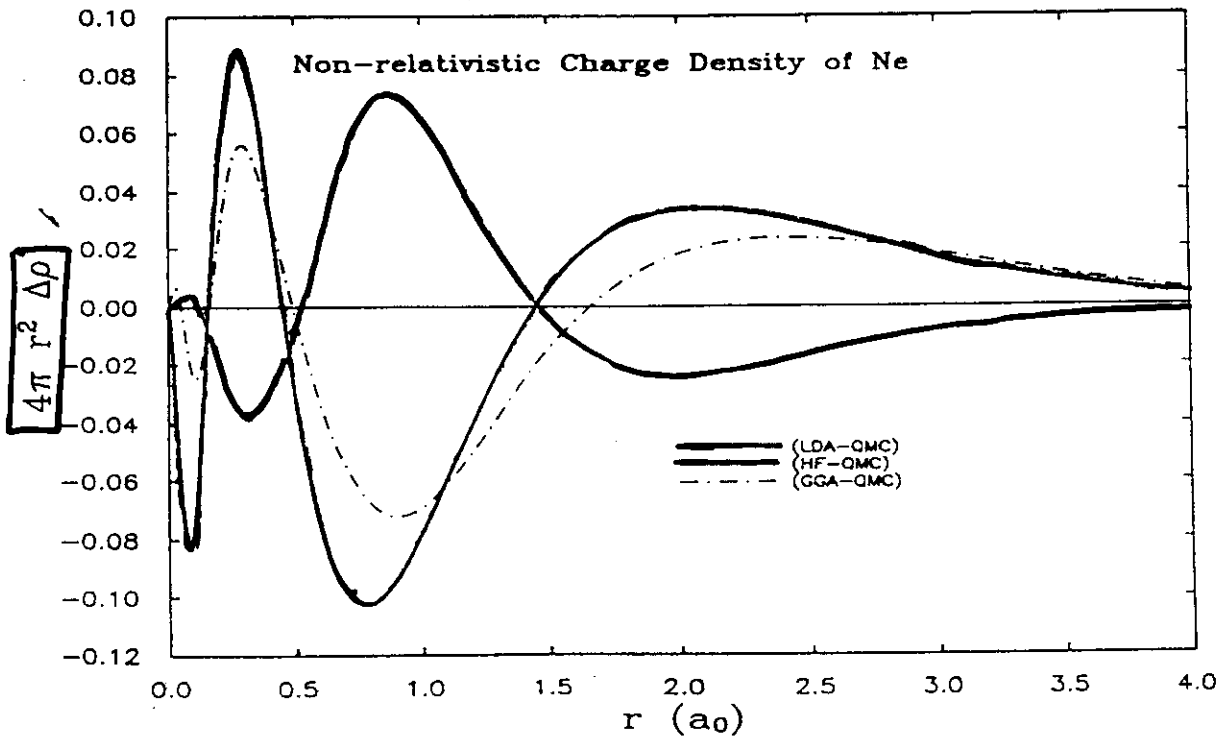

FIG. 2. Errors in the LDA, GGA, and Hartree-Fock densities for Ne.

C. I. Umrigar, X. Gonze
Conference on Concurrent Computing in the Physical Sciences 1993
Phys. Rev. A 50 3827 (1994)

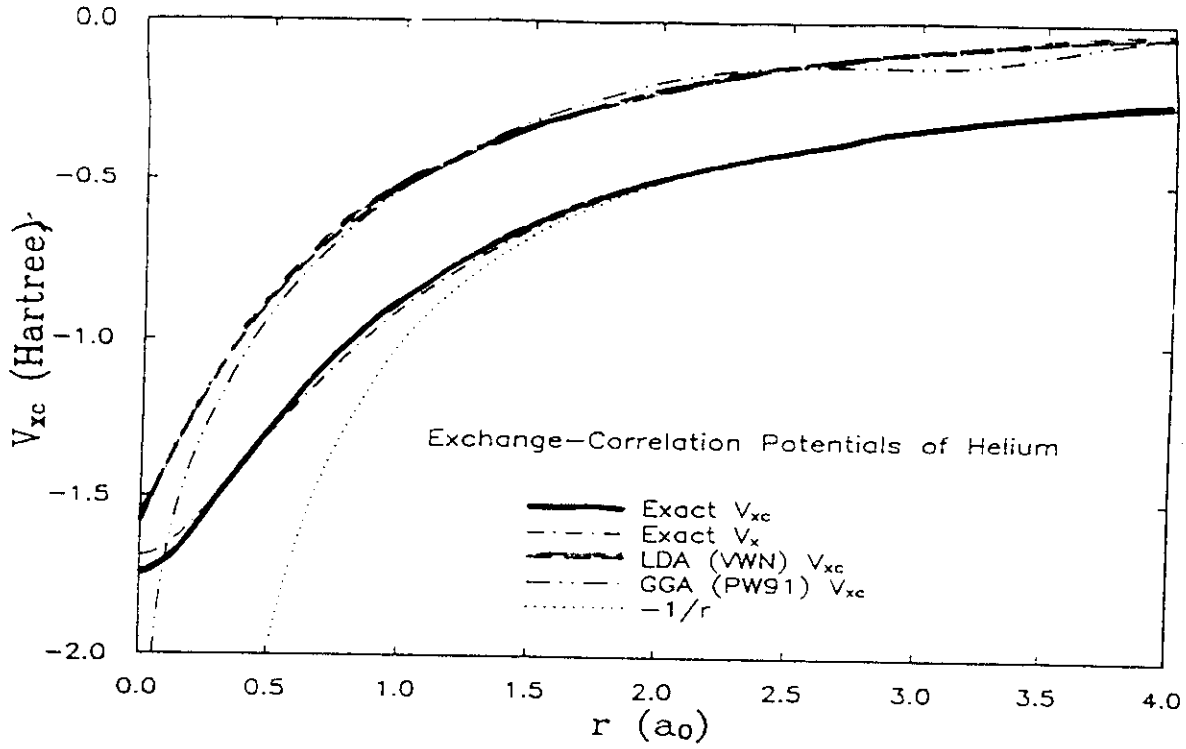

FIG. 3. Comparison of the LDA, and GGA v_{xc} with the exact v_{xc} and with v_x for He.

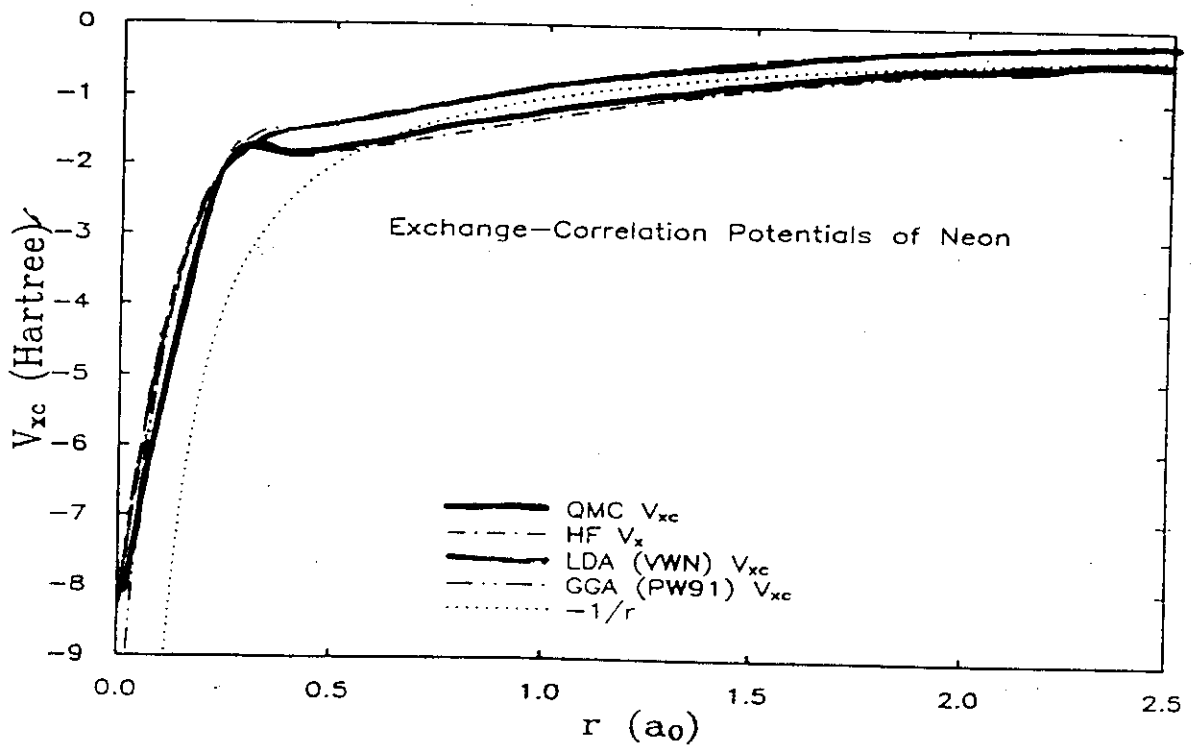

FIG. 4. Comparison of the LDA, and GGA v_{xc} with an accurate v_{xc} and with v_x for Ne.

C.J. Umrigar, X. Gonze

Conference on Concurrent Computing in the Physical Sciences 199?

Phys. Rev. A 50 3827 (1994)

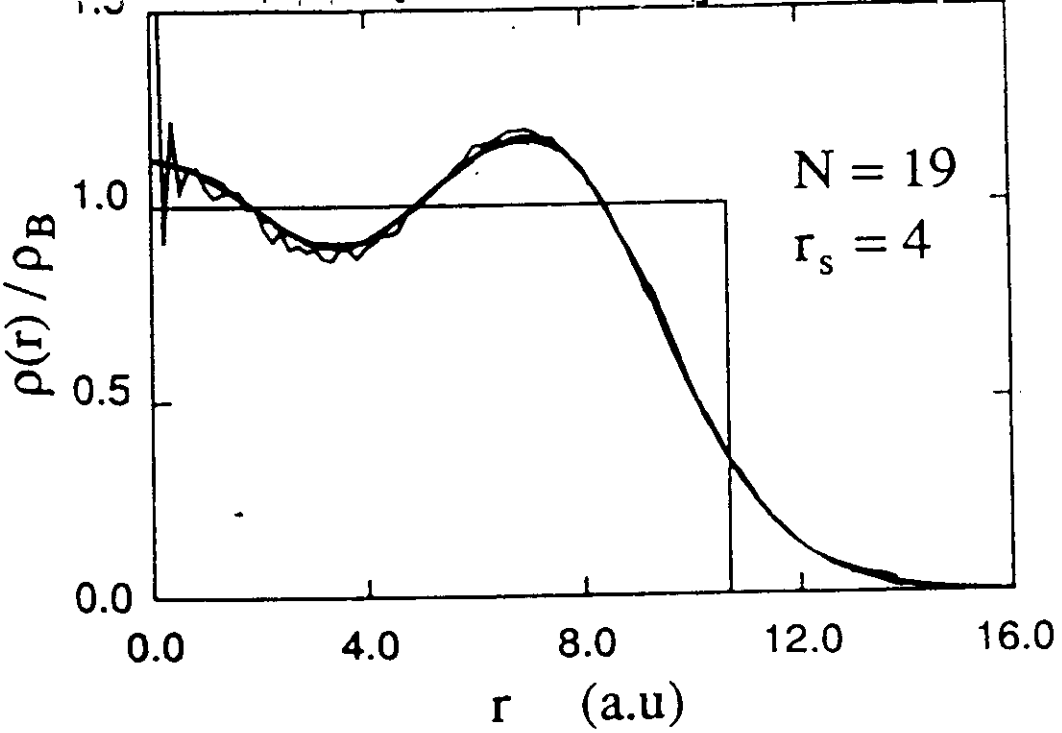

FIG. 1. Electron density $\rho(r)$ as a function of distance from the center of the jellium sphere. Solid line, VMC computation; dashed line, LSDA computation.

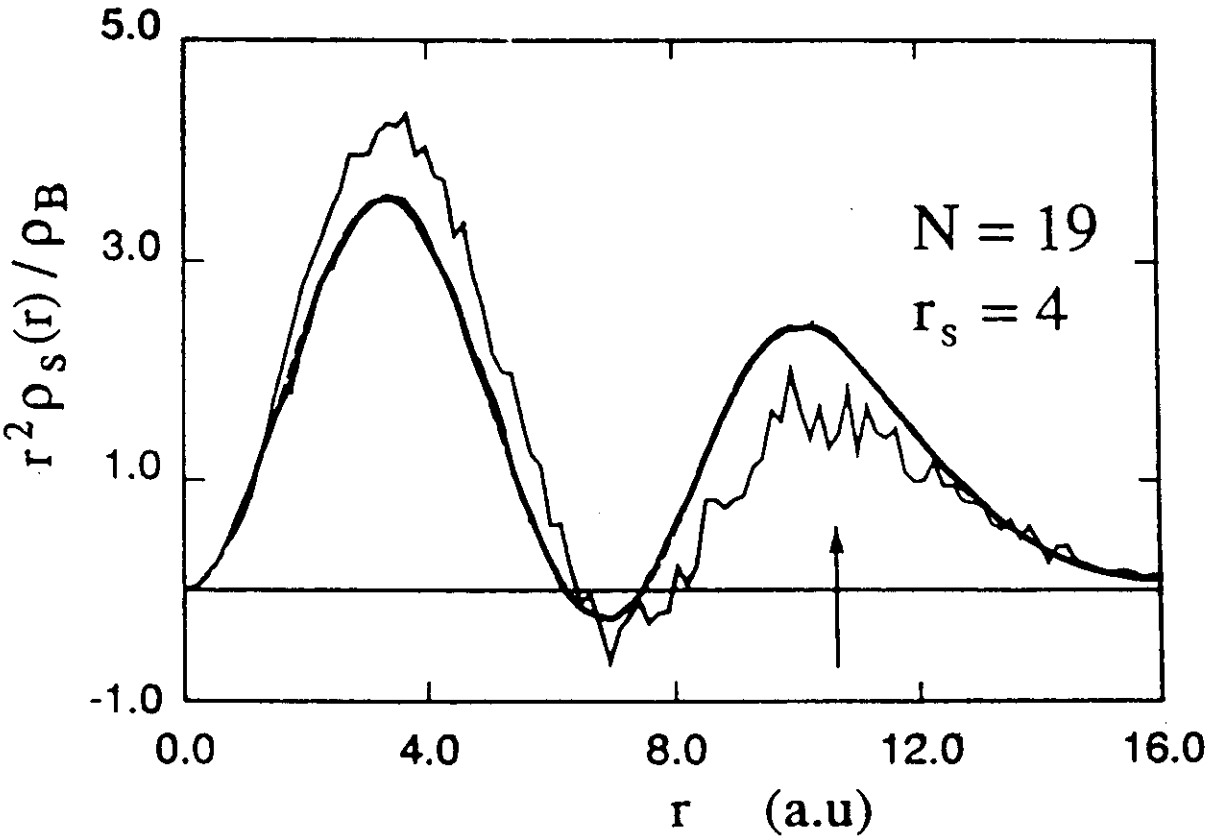

FIG. 2. Electron-spin density $\rho_s(r)$ times r^2 as a function of distance from the center of the jellium sphere. Solid line, VMC computation; dashed line, LSDA computation.

P. Ballone, C. Umrigar, P. Delaly Phys. Rev. B. 45 6293 (1992)

Atomic Ionization Energies

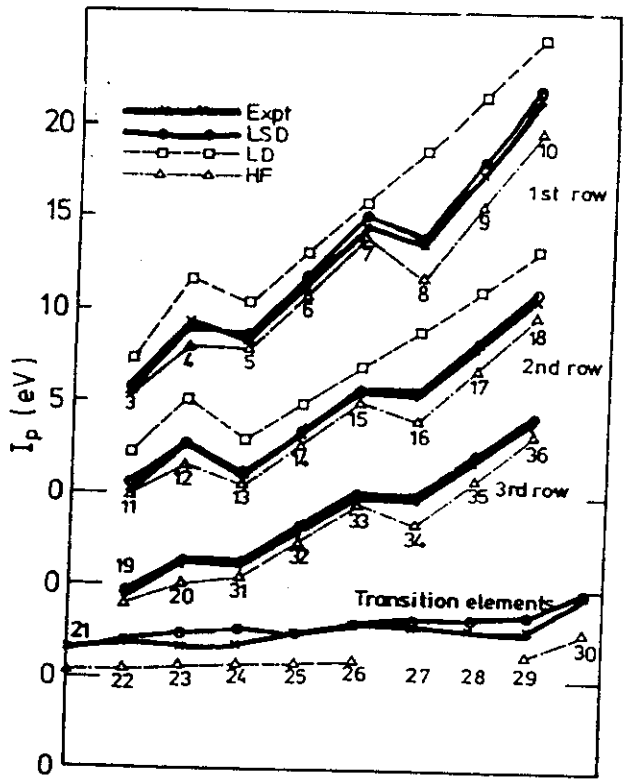

FIG. 8. First ionization energy of atoms in the local-density (LD), local spin-density (LSD), and Hartree-Fock (HF) approximations compared with experiment. The numbers show the atomic numbers of the atoms considered. For reasons of clarity, the zero of energy is shifted by 5, 10, and 15 eV for the second row, the third row, and the transition-element row, respectively. The LD results for the first and second rows are increased by an additional 2 eV.

R.O. Jones and O. Gunnarsson
Rev. Mod. Phys., Vol. 61, No. 3, July 1989

	I^{exp}	$I^{LSD-\Delta SCF}$	$I^{LSD-\nu}$	[eV]
Li	5.4	5.7	3.4	
Be	9.3	9.1	5.7	
B	8.3	8.8	4.2	
C	11.3	12.1	6.3	
N	14.5	15.3	6.5	
O	13.6	14.2	7.4	
F	17.4	18.4	10.5	
Ne	21.6	22.6	13.3	

TRANSITION ENERGIES

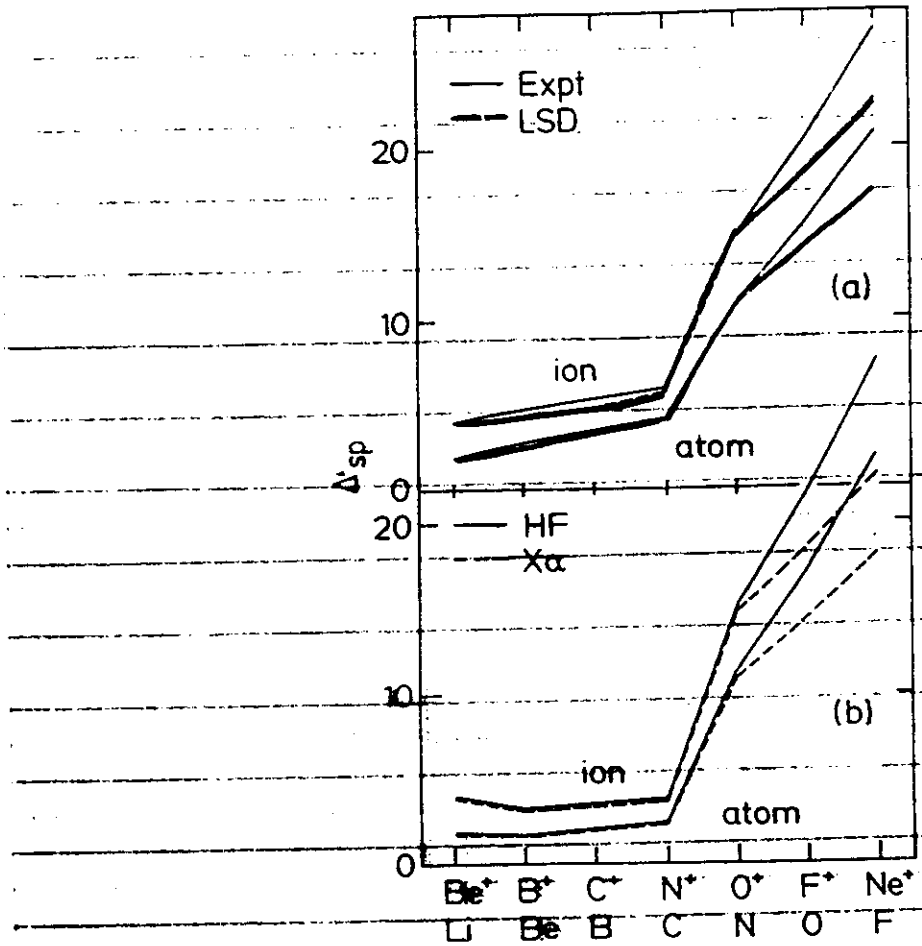

$\Delta_{sp} = E(1s^2 2s\, 2p^{n-1}) - E(1s^2 2s^2 2p^{n-2})$

$\Delta_{sd} = E([\text{core}]3d^{n-1}4s^1) - E([\text{core}]3d^{n-2}4s^2)$

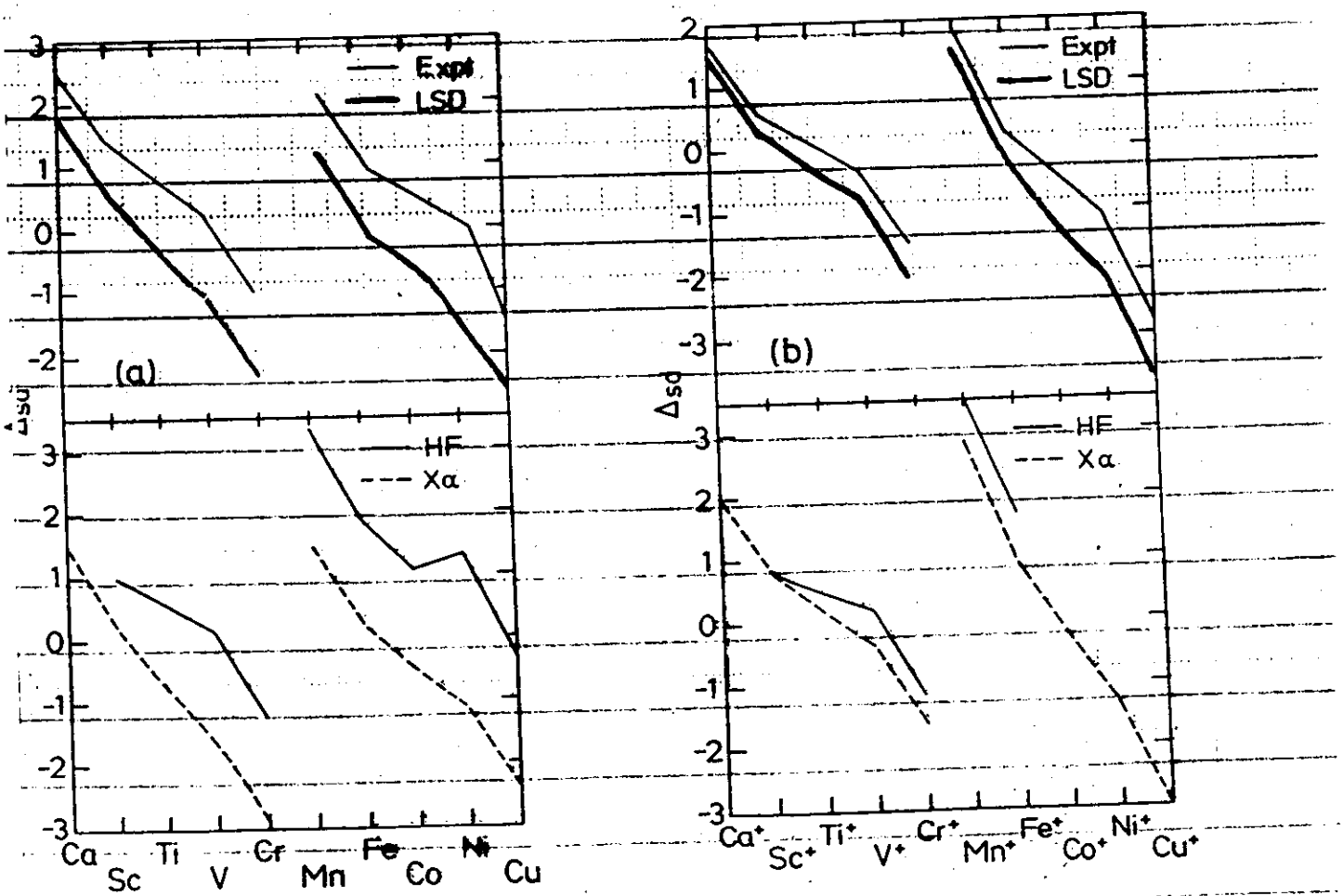

R.O. Jones and O. Gunnarsson

Rev. Mod. Phys., Vol. 61, No. 3, July 1989

Formal expression for $E_{xc}[n]$

$$\hat{H}^{(\lambda)} = \hat{T}_e + \lambda \hat{U} + \hat{V}_{ext}^{(\lambda)}$$

$$F_\lambda[n] = \min_{\Psi \to n} \langle \Psi | T + \lambda U | \Psi \rangle = \langle \Psi_\lambda | T + \lambda U | \Psi_\lambda \rangle$$

non-interacting electrons: $\lambda = 0$

$$F_0[n] = T_S[n]$$

interacting electrons: $\lambda = 1$

$$F_1[n] = F[n]$$

$$F[n] = T_S[n] + \int_0^1 d\lambda \, \frac{\partial F_\lambda}{\partial \lambda}$$

$$F[n] = T_S[n] + \int_0^1 d\lambda \, \langle \Psi_\lambda | U | \Psi_\lambda \rangle$$

$$F[n] = T_s[n] + \int_0^1 d\lambda \langle \psi_\lambda | U | \psi_\lambda \rangle$$

$$F[n] = T_s[n] + \int_0^1 d\lambda \int d^3r\, d^3r' \frac{e^2}{2} \frac{1}{|r-r'|} n(r) n(r') g(r,r',\lambda)$$

$g(r,r',\lambda)$ = pair correlation function with interaction λU

$g(r,r',\lambda) \to 1$ for $|r-r'| \to \infty$ $\forall \lambda$

$$F[n] = T_s[n] + \frac{e^2}{2} \int d^3r\, d^3r' \frac{n(r) n(r')}{|r-r'|} + \underbrace{\frac{e^2}{2} \int d^3r\, d^3r' \frac{n(r) n(r')}{|r-r'|} \int_0^1 d\lambda \left[g(r,r',\lambda) - 1 \right]}_{E_{xc}}$$

$$n_{xc}(r, r'-r) = n(r') \int_0^1 d\lambda \left[g(r,r',\lambda) - 1 \right]$$ exchange-correlation hole

$$\int n_{xc}(r, r'-r)\, d^3r' = -1$$

$$E_{xc} = \frac{e^2}{2} \int d^3r\, d^3r'\, n(r) \frac{1}{|r-r'|} n_{xc}(r, r'-r)$$

$$= \frac{e^2}{2} \int d^3r\, n(r) \int d^3s \frac{1}{|s|} n_{xc}(r, s)$$

Exchange-Correlation Hole in Atoms

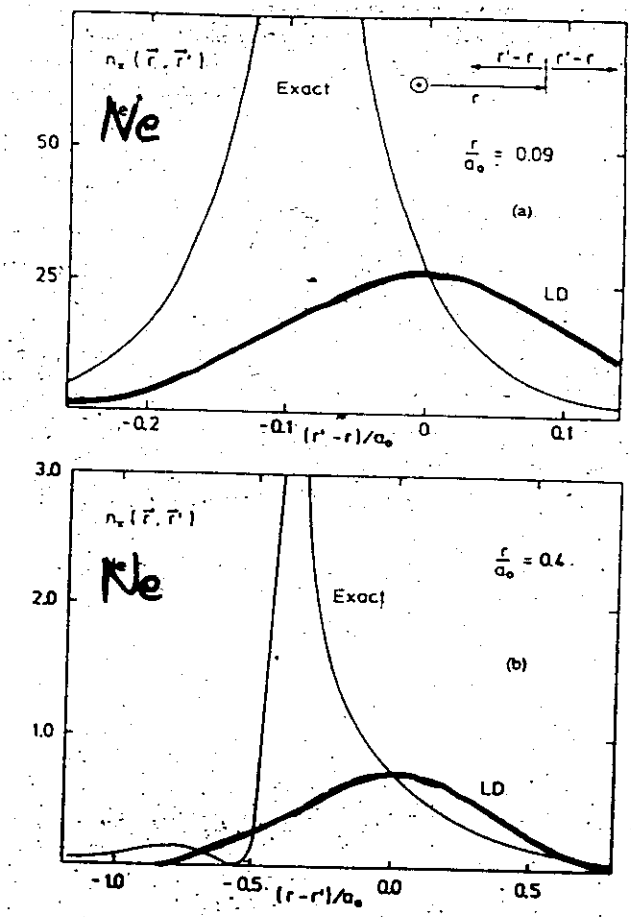

FIG. 5. Exchange hole $n_x(\vec{r},\vec{r}')$ for a neon atom. The full curves show exact results and the dashed curves show the results in the LD approximation. The curves in (a) and (b) are for two different values of r.

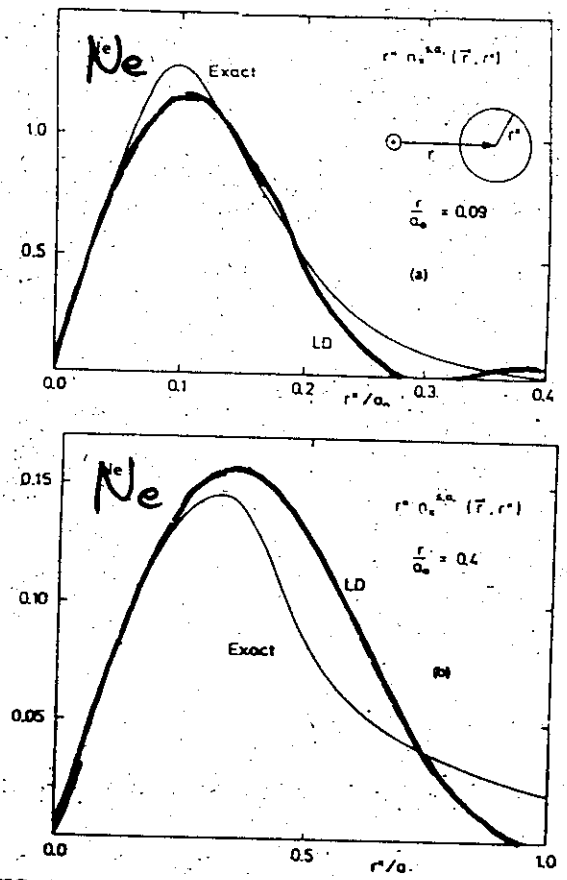

FIG. 7. Spherical average of the neon exchange hole [Eq. (17)] times r'' for (a) $r = 0.09$ a.u. and (b) $r = 0.4$ a.u. The full curves give the exact results and the dashed curves are obtained in the LD approximation.

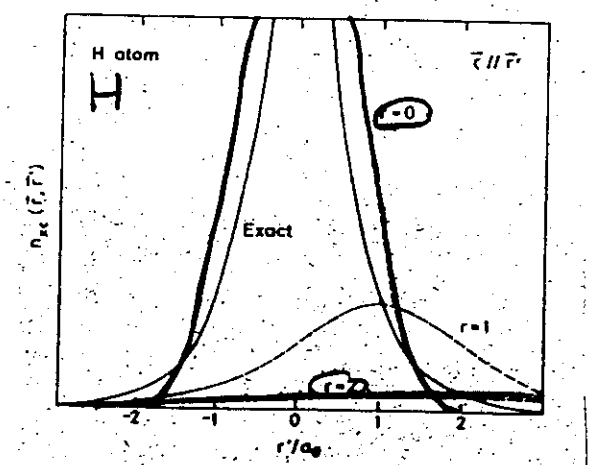

FIG. 4. Exchange-correlation hole $n_{xc}(\vec{r},\vec{r}')$ (Eq. 15) for a hydrogen atom. The full curve shows the exact hole, while the dashed curves depict the hole in the LD approximation [Eq. (16)] for various positions of the electron (0, 1, and 2 a.u. from the proton), using the dielectric function of Singwi *et al.* (Ref. 37). The x-axis gives the distance from the nucleus.

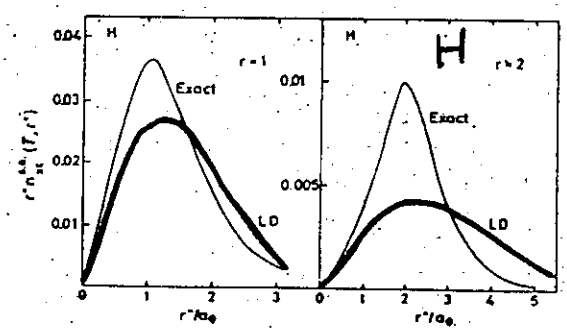

FIG. 6. Spherical average of the hydrogen XC hole [Eq. (16)] times r'' for $r = 1$ and 2 a.u. as a function of r''. The full curves give the exact results and the dashed curves are calculated in the LD approximation.

Phys. Rev. B20 3136 (1979)

First-Row Dimers

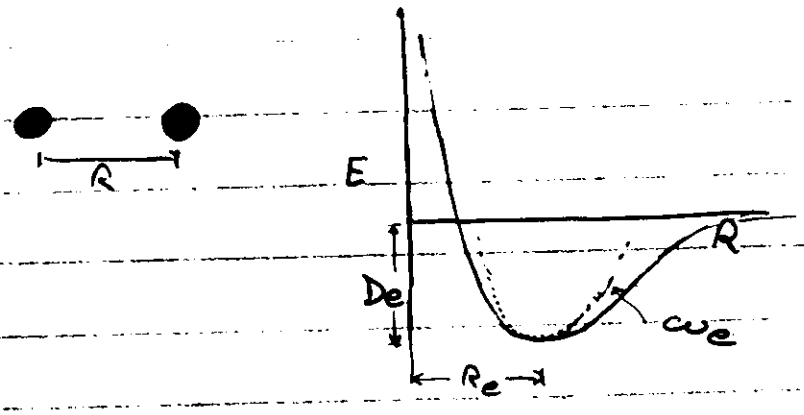

	R_e [a.u]		D_e [eV]		ω_e [cm^{-1}]		
	Exp	LSD	Exp	LSD	Exp	LSD	
H_2	1.40	1.45	4.75	4.91	4400	4277	
Li_2	5.05	5.12	1.06	1.01	351	347	
Be_2	4.71	4.63	0.11	0.50*0.4	294	362*	23%
B_2	3.04	3.03	3.08	3.93	1051	1082	
C_2	2.35	2.36	6.31	7.19	1857	1869	
N_2	2.07	2.08	9.91	11.34	2358	2387	
O_2	2.28	2.31	5.23	7.54*2.2	1580	1610	
F_2	2.68	2.62	1.66	3.32*1.7	892	1069*	19%

LSD G.S. Painter and F.W. Averill Phys. Rev. B 26 1781 (1982)

IB and IIB Dimers

		R_e [a.u.]		D_e [eV]		ω_e [cm^{-1}]	
		Exp	LSD	Exp	LSD	Exp	LSD
IB	Cu_2	4.20	4.07	1.97	3.18	265	295
	Ag_2	4.67	4.69	1.66	2.67	192	207
	Au_2	4.67	4.63	2.30	3.25	191	193
IIB	Zn_2	7.56	5.29*	0.06	0.23	—	78
	Cd_2	9.10	5.77*	0.05	0.24	—	62
	Hg_2	6.86	5.65*	0.07	0.23	—	71

LSD: P. Ballone and G. Galli, Phys. Rev. B 42 1112 (1990)

Cr_2	3.17	3.17 3.2	1.56 1.44	2.6 2.8	470	441 470

LSD: Baylard et al. Mol. Phys. 52 891 (1984)
Bernholc and Holzwarth Phys. Rev. Lett. 50 1451 (1983)

Crystalline Selenium

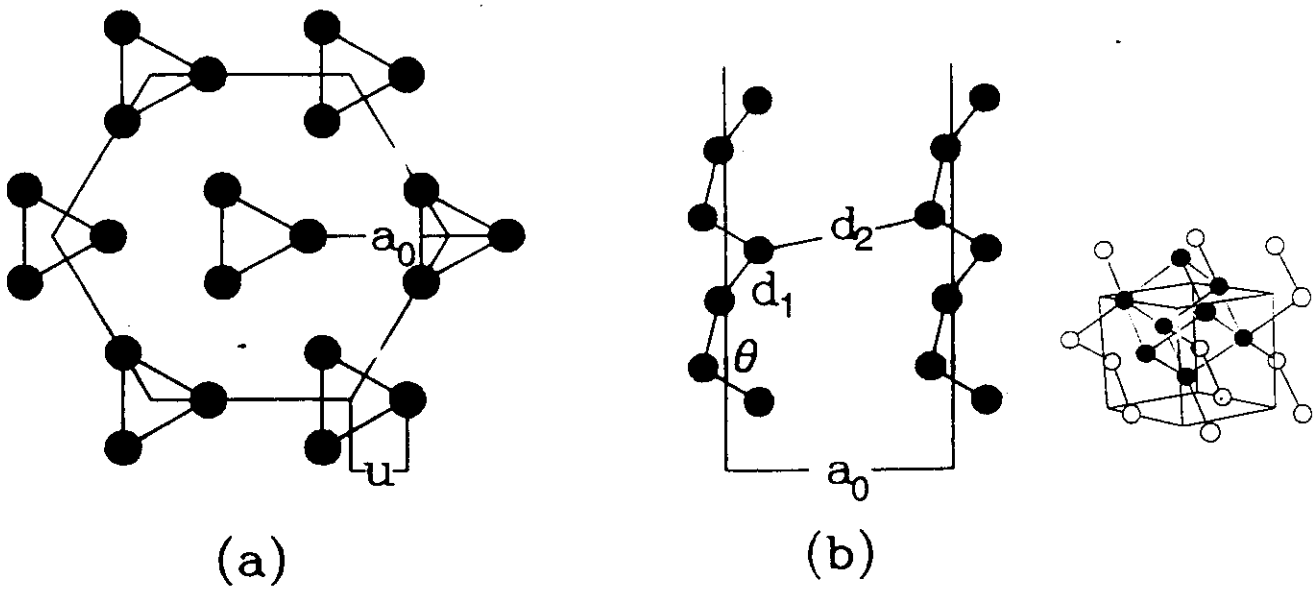

FIG. 1. Structure of selenium. (a) Projection on the basal plain of the selenium helices. a_0 is the length of the hexagonal edge, while u is the radius of the helices. (b) Side view of the chains: d_1 is the covalent (intrachain) bond length, while d_2 is the interchain bond length.

Lengths in a.u.

	d_1	d_2	θ	a_0	c	u	ua_0
LDA	4.61	5.84	103°	7.45	9.68	0.256	1.91
GC	4.57	6.60	105°	8.29	9.78	0.224	1.86
Expt.	4.51	6.45	102.7°	8.23	9.37	0.228	1.88

A. Dal Corso and R. Resta Phys. Rev. B 50 4327 (1994)

- Water, Ice..

- tendency to favour more homogeneous systems

- Overbinding of molecules and solids

-

- Good chemical trends

in good systems (covalent, metallic, ionic bonds bonding from region of high density)
- geometry is good
- bondlengths and angles within a few %
- phonons within a few %,
- dielectric, piezoelectric constant ~10 % too large

in bad systems: weakly bonded systems

much too short bondlengths, large overbinding

Atoms: $-\frac{e^2}{r}$, dissociation limit

Generalized Gradient Approximations (GGA)

Local Density Approximation

$$E_{xc}^{LDA}[n] = \int n(r)\, \varepsilon_{xc}^{hom}(n(r))\, d^3r$$

to go beyond LDA make a gradient expansion

$$E_{xc}^{GC}[n] = \int \left[n(r)\, \varepsilon_{xc}(n(r)) + C(n(r)) \frac{|\nabla n|^2}{n^{4/3}} + \dots \right] d^3r$$

- improves LDA for slowly varying density $\frac{|\nabla n|}{n} \ll 1$
- gives worse results for realistic systems
- sum-rules for $n_{xc}(r,r')$ are not fulfilled

GGA

$$E_{xc}^{GGA}[n] = \int n(r) \varepsilon_x(n(r))\, d^3r + \int F_{xc}[n(r), |\nabla n(r)|]\, d^3r$$

the correction function, F_{xc}, is chosen to satisfy formal conditions for the xc hole and fit to exact xc energies for atoms

NOT A UNIQUE RECIPE

$E_{xc}[\rho] = \int e_{xc}(\rho, \nabla\rho, \nabla^2\rho)\, d^3r$

$$k_F=(3\pi^2\rho)^{1/3},\quad k_s=\left(\frac{4}{\pi}k_F\right)^{1/2},\quad s=\frac{|\nabla\rho|}{2\,k_F\,\rho},$$

$$t=\frac{|\nabla\rho|}{2k_s\,\rho},\quad r_s=\left(\frac{3}{4\pi\rho}\right)^{1/3}.$$

All the parameters that appear in the following functionals are in atomic units.

LDA exchange functional:

$$e_x^{\mathrm{LDA}}=A_x\rho^{4/3}, \tag{A2}$$

where $A_x=-(3/4)(3/\pi)^{1/3}$.

LDA correlation functional (Perdew–Wang[13]):

$$e_c^{\mathrm{LDA}}=-2a\rho(1+\alpha_1 r_s)\times\log\left[1+\frac{1}{2a(\beta_1 r_s^{1/2}+\beta_2 r_s+\beta_3 r_s^{3/2}+\beta_4 r_s^2)}\right], \tag{A3}$$

where $a=0.031\,0907$, $\alpha_1=0.213\,70$, $\beta_1=7.5957$, $\beta_2=3.5876$, $\beta_3=1.6382$, and $\beta_4=0.492\,94$.

Langreth–Mehl exchange–correlation functional:[10]

$$e_x=e_x^{\mathrm{LDA}}-a\frac{|\nabla\rho|^2}{\rho^{4/3}}\left(\frac{7}{9}+18\,f^2\right), \tag{A4}$$

$$e_c=e_c^{\mathrm{RPA}}(\rho)+a\frac{|\nabla\rho|^2}{\rho^{4/3}}(2e^{-F}+18f^2), \tag{A5}$$

where $F=b|\nabla\rho|/\rho^{7/6}$, $b=(9\pi)^{1/6}f$, $a=\pi/(16(3\pi^2)^{4/3})$, and $f=0.15$.

Perdew–Wang '86 exchange functional:[14]

$$e_x=e_x^{\mathrm{LDA}}(\rho)\left(1+0.0864\frac{s^2}{m}+b\,s^4+c\,s^6\right)^m, \tag{A6}$$

where $m=1/15$, $b=14$ and $c=0.2$.

Perdew–Wang '86 correlation functional:[15]

$$e_c=e_c^{\mathrm{LDA}}(\rho)+e^{-\Phi}C_c(\rho)\frac{|\nabla\rho|^2}{\rho^{4/3}}, \tag{A7}$$

where

$$\Phi=1.745\,\tilde{f}\frac{C_c(\infty)}{C_c(\rho)}\frac{|\nabla\rho|}{\rho^{7/6}},$$

$$C_c(\rho)=C_1+\frac{C_2+C_3r_s+C_4r_s^2}{1+C_5r_s+C_6r_s^2+C_7r_s^3}, \tag{A8}$$

and $\tilde{f}=0.11$, $C_1=0.001\,667$, $C_2=0.002\,568$, $C_3=0.023\,266$, $C_4=7.389\times10^{-6}$, $C_5=8.723$, $C_6=0.472$, $C_7=7.389\times10^{-2}$.

Perdew–Wang '91 exchange functional:[11]

$$e_x=e_x^{\mathrm{LDA}}(\rho)\left\{\frac{1+a_1\,s\sinh^{-1}(a_2s)+(a_3+a_4e^{-100s^2})\,s^2}{1+a_1\,s\sinh^{-1}(a_2s)+a_5s^4}\right\}, \tag{A9}$$

where $a_1=0.196\,45$, $a_2=7.7956$, $a_3=0.2743$, $a_4=-0.1508$, and $a_5=0.004$.

Perdew–Wang '91 correlation functional:[11]

$$e_c=[e_c^{\mathrm{LDA}}(\rho)+\rho\,H(\rho,s,t)], \tag{A10}$$

where

$$H=\frac{\beta^2}{2\alpha}\log\left[1+\frac{2\alpha}{\beta}\frac{t^2+A\,t^4}{1+A\,t^2+A^2t^4}\right]+C_{c0}[C_c(\rho)-C_{c1}]t^2e^{-100\,s^2},$$

$$A=\frac{2\alpha}{\beta}[e^{-2\alpha\epsilon_c(\rho)/\beta^2}-1]^{-1},$$

and $\alpha=0.09$, $\beta=0.066\,726\,3212$, $C_{c0}=15.7559$, $C_{c1}=0.003\,521$. The function $C_c(\rho)$ is the same as for the Perdew–Wang '86 correlation functional. $\epsilon_c(\rho)$ is defined so that $e_c^{\mathrm{LDA}}(\rho)=\rho\epsilon_c(\rho)$.

Becke '88 exchange functional:[8]

$$e_x=e_x^{\mathrm{LDA}}(\rho)\left[1-\frac{\beta}{2^{1/3}A_x}\frac{x^2}{1+6\beta\,x\sinh^{-1}(x)}\right], \tag{A11}$$

where $x=2(6\pi^2)^{1/3}s=2^{1/3}|\nabla\rho|/\rho^{4/3}$, $A_x=(3/4)(3/\pi)^{1/3}$, and $\beta=0.0042$.

Wilson–Levy correlation functional:[12]

$$e_c=\frac{a\,\rho+b|\nabla\rho|/\rho^{1/3}}{c+d|\nabla\rho|/(\rho/2)^{4/3}+r_s} \tag{A12}$$

where $a=-0.748\,60$, $b=0.060\,01$, $c=3.600\,73$, and $d=0.900\,00$.

Closed shell Lee–Yang–Parr correlation functional:[16]

$$e_c=-a\frac{1}{1+d\,\rho^{-1/3}}\left\{\rho+b\,\rho^{-2/3}\left[C_F\,\rho^{5/3}-2t_W+\frac{1}{9}\times\left(t_W+\frac{1}{2}\nabla^2\rho\right)\right]e^{-c\,\rho^{-1/3}}\right\}, \tag{A13}$$

where

$$t_W=\frac{1}{8}\left(\frac{|\nabla\rho|^2}{\rho}-\nabla^2\rho\right), \tag{A14}$$

and $C_F=3/10(3\pi^2)^{2/3}$, $a=0.049\,18$, $b=0.132$, $c=0.2533$, and $d=0.349$.

[1] P. Hohenberg and W. Kohn, Phys. Rev. 136, B864 (1964).
[2] W. Kohn and L. J. Sham, Phys. Rev. 140, A1133 (1976).
[3] N. R. Kestner and O. Sinanoglu, Phys. Rev. 128, 2687 (1962).
[4] P. M. Laufer and J. B. Krieger, Phys. Rev. A 33, 1480 (1986).
[5] S. Kais *et al.*, J. Chem. Phys. 99, 417 (1993).
[6] M. Taut, Phys. Rev. A (in press).
[7] C. Umrigar and X. Gonze (unpublished).
[8] A. D. Becke, Phys. Rev. A 33, 3098 (1988).

TABLE IV. Known properties of the exact density functional

	Property	E_{xc}^{LDA} Ref. [8]	E_{xc}^{LM} Ref. [34]	E_{xc}^{PW91} Ref. [36]	E_{x}^{B88} Ref. [37]	E_{x}^{ECMV} Ref. [34]	E_{c}^{WL} Ref. [39]	E_{c}^{LYP} Ref. [40]
1	$\rho_x(\mathbf{r},\mathbf{r}') \le 0$	Y	-	Y	-	-	-	-
2	$\int \rho_x(\mathbf{r},\mathbf{r}')\,d\mathbf{r}' = -1$	Y	-	Y	-	-	-	-
3	$\int \rho_c(\mathbf{r},\mathbf{r}')\,d\mathbf{r}' = 0$	Y	-	Y	-	-	-	-
4	$E_x[\rho] < 0$	Y	Y	Y	Y	Y	-	-
5	$E_c[\rho] \le 0$	Y	N	N	-	-	N	N
6	$E_x[\rho]\,,\ E_{xc}[\rho] \ge -c\int \rho^{4/3}\,d\mathbf{r}$ [a]	Y	N	Y	Y	N	-	-
7	$E_x[\rho_\lambda] = \lambda E_x[\rho]$ [b]	Y	Y	Y	Y	Y	-	-
8	$E_c[\rho_\lambda] < \lambda E_c[\rho]\,,\ \lambda < 1$ [c]	Y	N	Y	-	-	N	N
9	$\lim_{\lambda\to\infty} E_c[\rho_\lambda] > -\infty$	N	Y [f]	Y [f]	-	-	Y	Y
10	$\lim_{\lambda\to 0} \frac{1}{\lambda} E_c[\rho_\lambda] > -\infty$	Y	N	Y	-	-	Y	Y
11	$\lim_{\lambda\to\infty} E_x[\rho^x_\lambda] > -\infty$ [c]	N	N	Y	N	N	-	-
12	$\lim_{\lambda\to 0} E_x[\rho^x_\lambda] > -\infty$	Y	N	Y	Y	Y	-	-
13	$\lim_{\lambda\to\infty} \frac{1}{\lambda} E_x[\rho^{xy}_\lambda] > -\infty$ [d]	Y	N	Y	Y	Y	-	-
14	$\lim_{\lambda\to 0} \frac{1}{\lambda} E_x[\rho^{xy}_{\lambda\lambda}] > -\infty$	N	N	Y	N	N	-	-
15	$\lim_{\lambda\to\infty} \lambda E_c[\rho^x_\lambda] > -\infty$	N	Y [f]	Y	-	-	N	N
16	$\lim_{\lambda\to 0} \frac{1}{\lambda} E_c[\rho^x_\lambda] = 0$	N	N	Y	-	-	N	N
17	$\lim_{\lambda\to\infty} E_c[\rho^{xy}_{\lambda\lambda}] = 0$	N	N	Y	-	-	N	N
18	$\lim_{\lambda\to 0} \frac{1}{\lambda^2} E_c[\rho^{xy}_{\lambda\lambda}] > -\infty$	N	Y [f]	Y	-	-	N	N
19	$\epsilon_x(r) \to -\frac{1}{2r},\ r\to\infty$	N	N	N	Y/N [g]	N	-	-
20	$v_x(r) \to -\frac{1}{r},\ r\to\infty$	N	N	N	N	N	-	-
21	$v_x(r), v_c(r) \to$ finite value, $r\to 0$	Y	N	N	N	N	N	N
22	LDA limit for constant $\rho(\mathbf{r})$	Y	N	Y	Y	Y	N	N

[a] $1.44 < c < 1.68$

[b] $\rho_\lambda(\mathbf{r}) = \lambda^3\rho(\lambda\mathbf{r})$; [c] $\rho^x_\lambda(\mathbf{r}) = \lambda\rho(\lambda x, y, z)$; [d] $\rho^{xy}_{\lambda\lambda}(\mathbf{r}) = \lambda^2\rho(\lambda x, \lambda y, z)$

[e] Note that $E_c[\rho_\lambda] < \lambda E_c[\rho]\,,\ \lambda < 1$ is equivalent to $E_c[\rho_\lambda] > \lambda E_c[\rho]\,,\ \lambda > 1$.

[f] But it diverges to $+\infty$

[g] "Y" for exponential $\rho(\mathbf{r})$, but "N" in general, *e.g.* $\epsilon_x^{B88}(r) \to -1/r$ for a gaussian.

GC (or GGA) vs LDA

- improves binding energies (better atomic energies)
  (but Be_2: exp = 0.11 eV LDA = 0.53 eV GC = 0.36 eV)
- bond lengths of IIA and IIB homonuclear dimers are much better
- water clusters and ice: much better geometries and energies
- Si, Ge, GaAs are better in LDA (not the binding energy)
- 4d-5d metals: it is not clear
- no improvement for the gap problem (nor for dielectric constants)

The improvement is not systematic and probably due to the wrong reasons.

GGA are fitted on atomic total xc energies: locally they are not better than LDA

They do not satisfy known asymptotic behaviour

In an atom:

$V_{xc} \underset{r\to\infty}{\sim} -\frac{e^2}{r}$ while $V_{xc}^{LDA,GGA}$ vanishes exponentially

$V_{xc} \underset{r\to 0}{\Longrightarrow}$ const while $V_{xc}^{LDA} \underset{r\to 0}{=}$ const

$V_{xc}^{GGA} \underset{r\to 0}{=} -\infty$

MICROSCOPIC FORMULATION

$$\overline{W} = \overline{W}_0 + \frac{\Omega}{2}\alpha\lambda^0\alpha + \frac{1}{2}\sum_{sl} u_{(s)}\Phi_{sl}u_{sl} - \frac{\Omega}{8\pi}E\epsilon_\infty E$$
$$-\Omega E\gamma^0\alpha - \Omega\sum_s u_{(s)}\Delta_{(s)}\alpha - e\sum_s EZ^*_{(s)}u_{(s)}$$

$$F_{(s)} = -\frac{\partial\overline{W}}{\partial u_{(s)}} = -\sum_{sl}\Phi_{sl}u_{sl} + \Omega\Delta_{(s)}\alpha + eZ^*_{(s)}E$$

$$\sigma = -\frac{1}{\Omega}\frac{\partial\overline{W}}{\partial\alpha} = -\lambda_0\alpha + \gamma_0 E + \sum_s \Delta_{(s)}u_{(s)}$$

$$F_{(s)} = 0$$

$$\Downarrow$$

$$\epsilon_0 = \epsilon_\infty + \frac{4\pi e^2}{\Omega}\frac{Z^{*2}}{\mu\omega^2_{TO}}$$

$$\lambda_{11} = \lambda^0_{11}, \quad \lambda_{12} = \lambda^0_{12} \quad \lambda_{44} = \lambda^0_{44} - \Omega\frac{\Delta^2_{14}}{\mu\omega^2_{TO}}$$

$$\gamma_{14} = \gamma^0_{14} + Z^* e\frac{\Delta_{14}}{\mu\omega^2_{TO}}$$

Two independent perturbations ($\alpha = 0$):

- $E \neq 0, u_{(s)} = 0$: $F_{(s)} \Rightarrow Z^*$; $\sigma \Rightarrow \gamma^0_{14}$
- $u_{(s)} \neq 0, E = 0$: $F_{(s)} \Rightarrow \omega^2_{TO}$; $\sigma \Rightarrow \Delta_{14}$

Lattice Dynamics

- Adiabatic Approximation

$$H = T_{ion} + E(\{\mathbf{R}_{ls}\})$$

- Harmonic Approximation $(\mathbf{R}_{ls} = \mathbf{R}^0_{ls} + \mathbf{u}_{l,s})$

$$E(\{\mathbf{R}_{ls}\}) = E(\{\mathbf{R}^0_{ls}\}) + \sum_{ls} C_{ls}\mathbf{u}_{l,s} + \frac{1}{2}\sum_{ls}\sum_{l's'} \mathbf{u}_{l's'} C_{lsl's'} \mathbf{u}_{ls} + \ldots$$

$$C_{ls} = \left.\frac{\partial E}{\partial \mathbf{u}_{ls}}\right|_0 = 0 \qquad C_{lsl's'} = \left.\frac{\partial^2 E}{\partial \mathbf{u}_{ls}\partial \mathbf{u}_{l's'}}\right|_0$$

- Equation of Motion $\Rightarrow$ Dynamical Matrix

$$M_s\ddot{\mathbf{u}}_{ls} = -\frac{\partial E}{\partial \mathbf{u}_{ls}} = -\sum_{l',s'} C_{lsl's'}\mathbf{u}_{l's'}$$

$$\mathbf{u}_{ls} = \frac{\mathbf{v}_s(\mathbf{q})}{\sqrt{M_s}}\, e^{i\mathbf{q}\mathbf{R}_l - i\omega t} \Rightarrow \omega^2 \mathbf{v}_s = \sum_{s'} D_{ss'}(\mathbf{q})\mathbf{v}_{s'}$$

$$D_{ss'}(\mathbf{q}) = \sum_{l'} C_{lsl's'}\, \frac{e^{i\mathbf{q}(\mathbf{R}_{l'} - \mathbf{R}_l)}}{\sqrt{M_s M_{s'}}}$$

PW-PP S. Baroni, P. Giannozzi, A. Testa Phys. Rev. Lett 58 1861 (1987)
X. Gonze, D.C. Allen, M.P. Teter Phys. Rev. Lett 68 3603 (1992)

LMTO S.Y. Savrasov Phys. Rev. Lett. 69 2819 (1992)

LAPW G.Z. Wang, R. Yu, H. Krakauer Phys. Rev. Lett. 72 368 (1994)

S. dG
P. Pavone
A. Dal Corso
M. Buongiorno Nardelli
C. Bungaro
A. Debernardi
N. Vast
G. Roma
A.M. Saitta

Lattice Dynamics & Linear-Response

$$M_s \ddot{\mathbf{u}}_{ls} = -\sum_{l',s'} C_{lsl's'} \mathbf{u}_{l's'}$$

within Density Functional Theory

$$E(\{\mathbf{R}_{ls}\}) = \min\left\{ \mathrm{F[n]} + \int \mathrm{n}(\mathbf{r}) \mathrm{V}^{\mathrm{ion}}_{\{\mathbf{R}_{ls}\}}(\mathbf{r}) d\mathbf{r} \right\} + \mathrm{E}^{\mathrm{ion}}$$

$$\underbrace{\frac{\partial E(\{\mathbf{R}_{ls}\})}{\partial u_{ls}} = \int n(\mathbf{r}) \frac{\partial \mathrm{V}^{\mathrm{ion}}_{\{\mathbf{R}_{ls}\}}}{\partial u_{ls}}(\mathbf{r})\, d\mathbf{r} + \frac{\partial E^{\mathrm{ion}}}{\partial u_{ls}}}_{\text{Helmann-Feynman theorem}}$$

$$\Downarrow$$

$$C_{lsl's'} = \left. \frac{\partial^2 E(\{\mathbf{R}_{ls}\})}{\partial u_{ls} \partial u_{l's'}} \right|_0$$

$$= \int \left[\left. \frac{\partial n}{\partial u_{ls}} \right|_0 \left. \frac{\partial \mathrm{V}^{\mathrm{ion}}_{\{\mathbf{R}_{ls}\}}}{\partial u_{l's'}} \right|_0 + n \left. \frac{\partial^2 \mathrm{V}^{\mathrm{ion}}_{\{\mathbf{R}_{ls}\}}}{\partial u_{ls} \partial u_{l's'}} \right|_0 \right] d\mathbf{r} + \left. \frac{\partial^2 E^{\mathrm{ion}}}{\partial u_{ls} \partial u_{l's'}} \right|_0$$

Density-Functional Perturbation Theory

DFT

$$V_{\rm SCF}(\mathbf{r}) = V_{\rm ion}(\mathbf{r}) + e^2 \int \frac{n(\mathbf{r}')}{|\mathbf{r}-\mathbf{r}'|} d\mathbf{r}' + \mu_{\rm xc}\left(n(\mathbf{r})\right)$$

$$\left(-\nabla^2 + V_{\rm SCF}(\mathbf{r})\right) \psi_v(\mathbf{r}) = \epsilon_v \psi_v(\mathbf{r})$$

$$n(\mathbf{r}) = 2 \sum_{\epsilon_v < \epsilon_F} |\psi_v(\mathbf{r})|^2$$

DFPT

$$\Delta V_{\rm SCF}(\mathbf{r}) = \Delta V_{\rm ion}(\mathbf{r}) + e^2 \int \frac{\Delta n(\mathbf{r}')}{|\mathbf{r}-\mathbf{r}'|} d\mathbf{r}' + \mu'_{\rm xc}\left(n(\mathbf{r})\right) \Delta n(\mathbf{r})$$

$$\left(-\nabla^2 + V_{\rm SCF}(\mathbf{r}) - \epsilon_v\right) \Delta\psi_v(\mathbf{r}) = -P_c \Delta V_{\rm SCF}(\mathbf{r}) \psi_v(\mathbf{r})$$

$$\Delta n(\mathbf{r}) = 4 \sum_{\epsilon_v < \epsilon_F} \psi_v^*(\mathbf{r}) \Delta\psi_v(\mathbf{r})$$

S.Baroni, P.Giannozzi and A.Testa, *Phys.Rev.Lett.* 58, 1861 (1987)

P.Giannozzi, S.de Gironcoli, P.Pavone, and S.Baroni, *Phys.Rev.* B43, 7231 (1991)

Allows to treat perturbations of any periodicity

$$R + \tau_s \rightarrow R + \tau_s + u_s(R)$$

$$u_s(R) = u_s(q)\, e^{+iqR}$$

$$\Delta V^q_{ion}(r) = \sum_R \frac{\partial V_s(r - R - \tau_s)}{\partial \tau_s} \cdot u_s(q)\, e^{+iqR}$$

$$\Delta V^q_{ion}(r+R) = e^{+iqR}\, \Delta V^q_{ion}(r) \qquad \Delta V^q_{ion}(r) = e^{+iqr}\, \underbrace{\Delta \tilde{V}^q_{ion}(r)}_{\text{periodic}}$$

$$\Delta \psi^{(q)}_{kv}(r) = \sum_{c \neq v} \frac{\varphi_{k+qc}(r) \, \langle \varphi_{k+qc} | \Delta V^q | \varphi_{kv} \rangle}{\varepsilon_{kv} - \varepsilon_{k+qc}}$$

is a Bloch state at $k+q$

$$\Delta n^q(r) = 4 \sum_{v\,k} \varphi^*_{kv}(r)\, \Delta \psi^{(q)}_{kv}(r)$$

$$\Delta n^q(r+R) = e^{+iqR}\, \Delta n^q(r) \qquad \Delta n^q(r) = e^{+iqr}\, \underbrace{\Delta \tilde{n}^q(r)}_{\text{periodic}}$$

$$\Delta V^q_{ks}(r) = \Delta V^q_{ion}(r) + e^2 \int \frac{\Delta n^q(r')}{|r - r'|} d^3r + \mu'_{xc}(n(r))\, \Delta n^q(r)$$

$$\Delta V^q_{ks}(r+R) = e^{+iqR}\, \Delta V^q_{ks}(r) \qquad \Delta V^q_{ks}(r) = e^{+iqr}\, \underbrace{\Delta \tilde{V}^q_{ks}(r)}_{\text{periodic}}$$

Analytic $q \to 0$ limit

Electric field $\quad E \sim \lim_{q \to 0} E e^{+iqr}$

$$\Delta V_E = eEr \sim \lim_{q \to 0} eE \frac{e^{+iqr}}{iq}$$

$$D = E + 4\pi P$$

$$D = \varepsilon_\infty E$$

$$\Delta V_{KS} = eD \frac{e^{+iqr}}{iq} + \sum_G \frac{4\pi e^2 \Delta n(q+G)}{(q+G)^2} e^{+i(q+G)r} + \mu'_{xc}(n(r)) \Delta n^q(r)$$

$$\Delta V_{KS} = e\left[D - 4\pi e \frac{\Delta n(q)}{iq}\right] \frac{e^{+iqr}}{iq} + \sum_{G \neq 0} \cdots + \mu'_{xc} \Delta n^q$$

$$\begin{cases} \Delta n(q) = \Delta n(-q)^* \\ \Delta n(0) = 0 \end{cases} \Rightarrow e\Delta n(q) = iqP + \cdots \quad \text{for } -\nabla P = \rho_{ind}$$

$$\Delta V_{KS} = eE \frac{e^{+iqr}}{iq} + \Delta V'_{KS}$$

$$\Delta \psi^q_{k\sigma} = \sum_c \frac{\phi_{k+qc} \quad \langle \phi_{k+qc} | \Delta V_{KS} | \phi_{k\sigma} \rangle}{\varepsilon_{k\sigma} - \varepsilon_{k+qc}}$$

$$\langle \phi_{k+qc} | \frac{e^{+iqr}}{iq} | \phi_{k\sigma} \rangle = \frac{\langle \phi_{k+qc} | \vec{p}\, e^{+iqr} | \phi_{k\sigma} \rangle}{\varepsilon_{k\sigma} - \varepsilon_{k+qc}}$$

$\lim_{q \to 0}$

$$\Delta V^q_{KS} \to \{E, \Delta V'_{KS}\}$$

$$\Delta \psi^q_{k\sigma} \to \{\Delta \psi_E, \Delta \psi_{V'}\}$$

$$\Delta n^q \to \{P, \Delta n'\}$$

DYNAMICAL and DIELECTRIC PROPERTIES

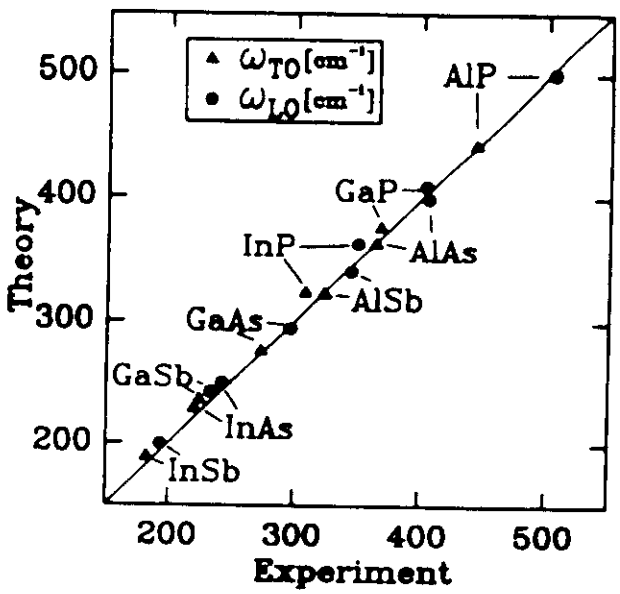

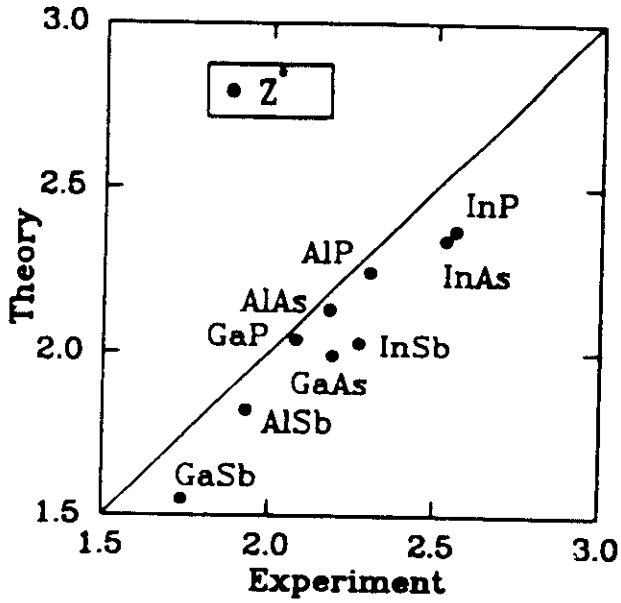

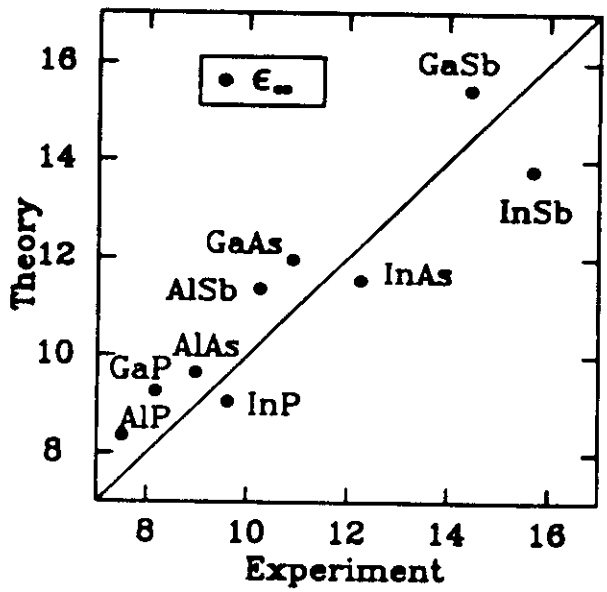

III-V

II-VI	ω_{TO}	ω_{LO}	Z^*	ϵ_∞
ZnS	317 (274)	379 (349)	1.92 (2.01)	5.11 (5.1)
ZnSe	235 (207)	273 (250)	1.91 (1.91)	6.29 (5.6)
ZnTe	198 (–)	221 (–)	1.85 (2.0)	7.77 7.3

PIEZOELECTRIC CONSTANTS

II-VI

$\bar{\gamma}_{14}$	S	Se	Te
Zn	0.27 (0.27)	0.10 (0.10)	− 0.10 (0.07)

III-V

$\bar{\gamma}_{14}$	P	As	Sb
Al	0.11 (−)	− 0.03 (−)	− 0.13 (−0.16)
Ga	− 0.18 (−0.18)	− 0.35 (−0.32)	− 0.40 (−0.39)
In	0.12 (|0.09|)	− 0.08 (−0.10)	− 0.20 (−0.18)

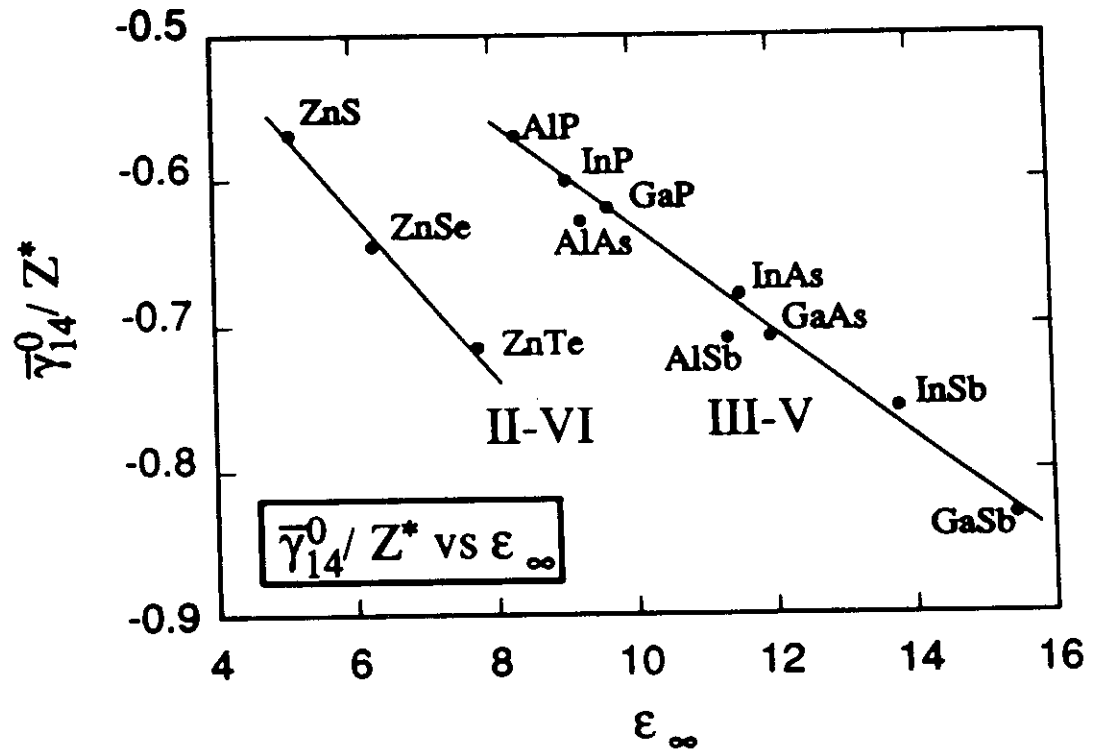

Lattice Dynamical Properties

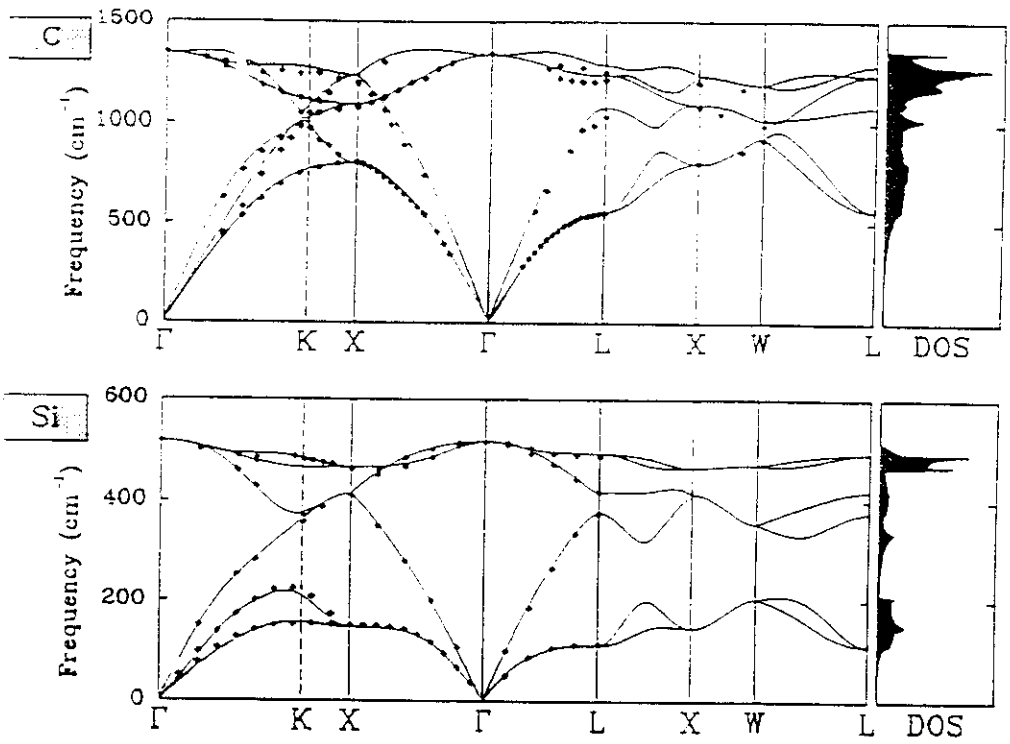

P. Giannozzi, S. de Gironcoli, P. Pavone and S. Baroni PRB 43 7231 (91

Thermal Expansion

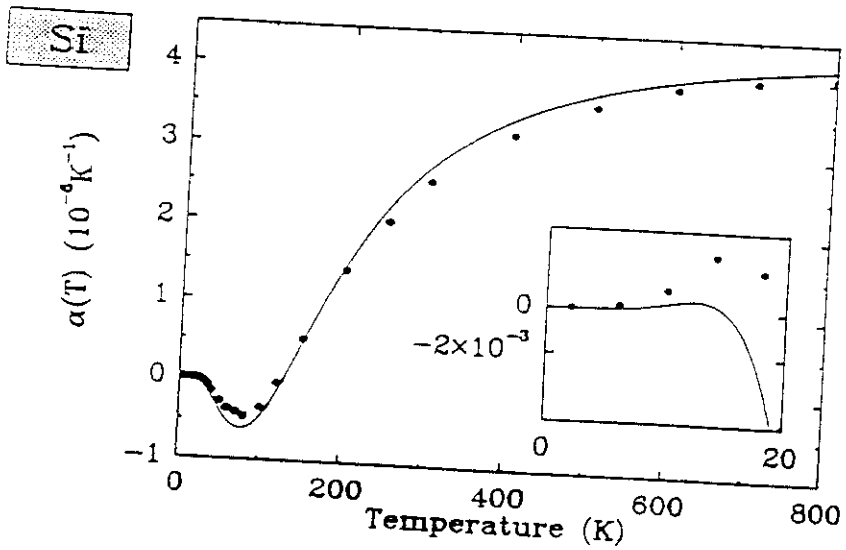

P. Pavone SISSA - PhD Thesis 1991

The quasi-harmonic approximation

At $T = 0$ the atomic equilibrium positions in a crystal are defined by the minimum of the potential energy $U(T = 0, V)$. At finite temperature and in the absence of an applied pressure the equilibrium condition requires the minimization of the appropriate thermodynamical potential, in this case the Helmholtz free energy defined as:

$$F(T, V) = U(T, V) - T\,S(T, V)\ , \tag{3.1}$$

where $S(T, V)$ is the entropy of the crystal. In the harmonic approximation the crystal can be considered as a collection of independent harmonic oscillators, so that the Helmholtz free energy can be expressed in terms of vibrational quantities only:

$$F_{\rm har}(T, V) = F^0(V) + F_{\rm vib}(T, V)\ . \tag{3.2}$$

The term $F^0(V)$ in Eq. (3.2) corresponds to the free energy at $T = 0$ and can be written in the following way:

$$F_0(V) = \mathcal{E}(V) + U^0_{\rm vib}(V)\ , \tag{3.3}$$

where $\mathcal{E}(V)$ is the internal energy of the static lattice at volume V, i.e. the so-called *total* energy which can be evaluated with the methods described in Chapter 1, and $U^0_{\rm vib}(V)$ is the zero-point vibrational energy. On the other hand, the vibrational contribution in the harmonic approximation is given by:

$$F_{\rm vib}(T, V) = k_B T \sum_{n,\mathbf{q}} \ln\left[1 - \exp\left(-\frac{\hbar\omega_n(\mathbf{q}, V)}{k_B T}\right)\right]\ .$$

This approximation is known as the *Quasi-Harmonic Approximation.*

P. Pavone SISSA - PhD Thesis 1991

Phonon Dispersions in White and Grey Tin

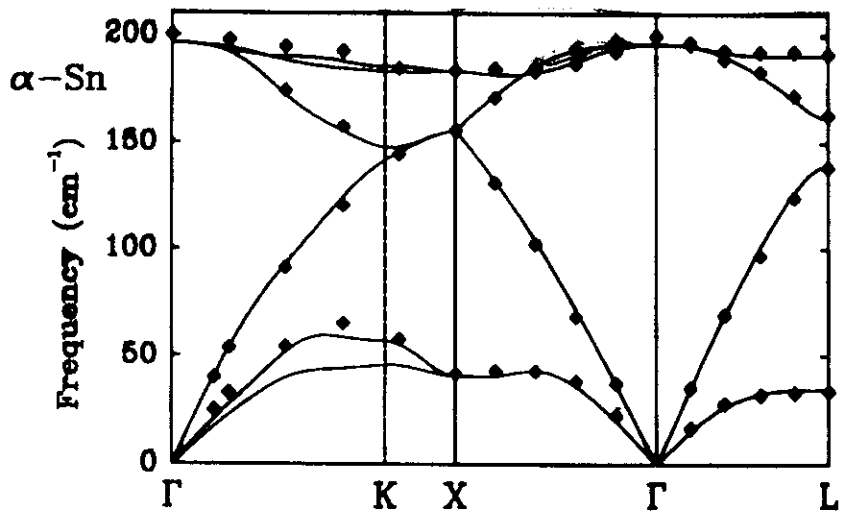

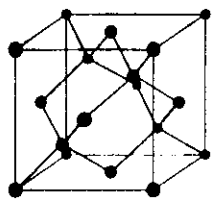

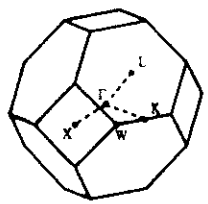

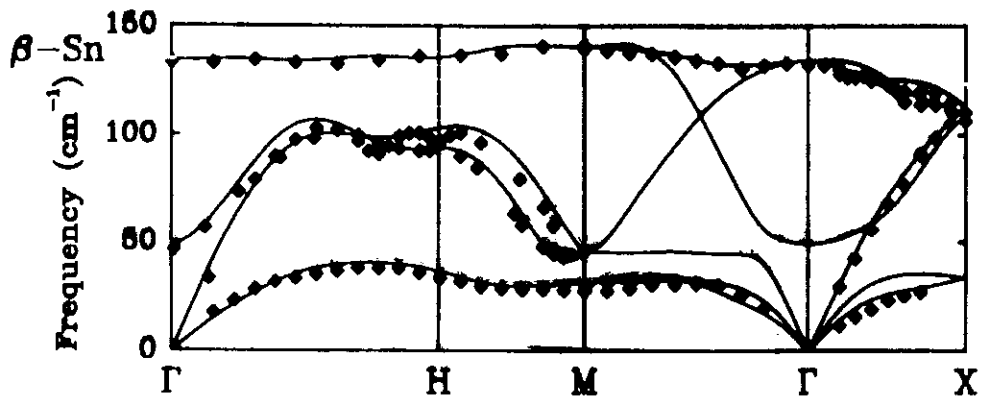

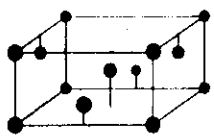

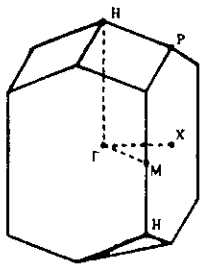

The Mechanism of the Transition

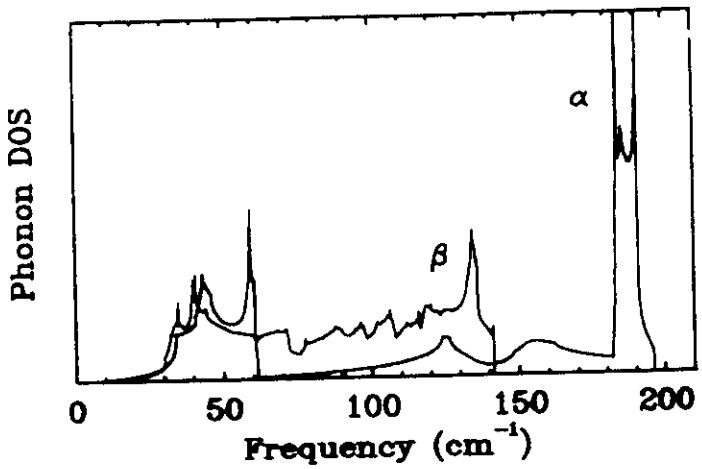

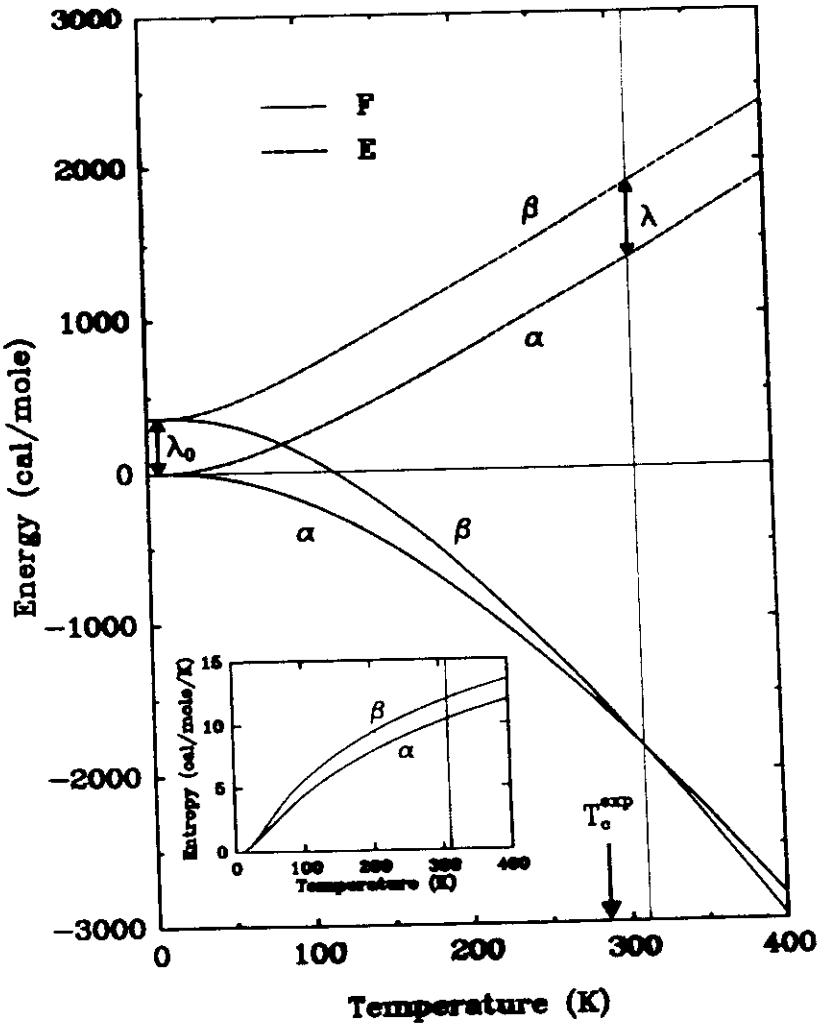

Stefano Baroni

SISSA-Trieste / CECAM-Lyon

Substitutional Disorder as a Perturbation

Pseudobinary Alloy: $A_x\ B_{1-x}\ C$

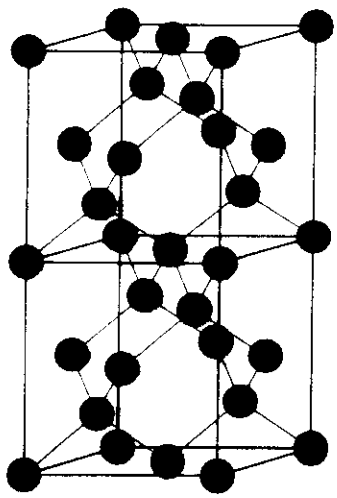

Configurational variables

$$\{\sigma_{\mathbf{R}}\} = \begin{cases} +1 & \text{if A in } \mathbf{R} \\ -1 & \text{if B in } \mathbf{R} \end{cases}$$

External potential

$$V_{ext}(\mathbf{r}) = \underbrace{\sum \left(\frac{1}{2}(v_A + v_B)(\mathbf{r} - \mathbf{R}) \right) + v_C(\mathbf{r} + \mathbf{t} - \mathbf{R})}_{V_0(\mathbf{r})}$$

$$+ \quad \underbrace{\sum \sigma_{\mathbf{R}} \left(\frac{1}{2}(v_A - v_B)(\mathbf{r} - \mathbf{R}) \right)}_{\Delta V(\mathbf{r}) \equiv \sum \sigma_{\mathbf{R}} \Delta v(\mathbf{r} - \mathbf{R})}$$

$$V_{ext}(\{\sigma_{\mathbf{R}}\}, \mathbf{r}) \longrightarrow n(\{\sigma_{\mathbf{R}}\}, \mathbf{r}) \longrightarrow E(\{\sigma_{\mathbf{R}}\})$$

Mapping the Alloy onto a Lattice Gas

Perturbation theory:

$$H = H_0 + \lambda \Delta V$$

$$\overbrace{\frac{\partial E_\lambda}{\partial \lambda} = \int n_\lambda(\mathbf{r}) \Delta V(\mathbf{r}) d\mathbf{r}}^{\text{Hellmann-Feynman theorem}} \quad \Longrightarrow \frac{\partial^2 E_\lambda}{\partial \lambda^2} = \int \frac{\partial n_\lambda(\mathbf{r})}{\partial \lambda} \Delta V(\mathbf{r}) d\mathbf{r}$$

$$E_\lambda = E_0 + \lambda \int n_0(\mathbf{r}) \Delta V(\mathbf{r}) d\mathbf{r} + \frac{\lambda^2}{2} \int \Delta V(\mathbf{r}) \left. \frac{\partial n_\lambda(\mathbf{r})}{\partial \lambda} \right|_0 + \mathcal{O}\left(\lambda^3\right)$$

The lattice gas:

$$\begin{aligned} \Delta E(\{\sigma\}) &= \sum_{\mathbf{R}} \sigma_{\mathbf{R}} \underbrace{\int n_0(\mathbf{r}) \Delta v(\mathbf{r} - \mathbf{R}) d\mathbf{r}}_{\Delta \mu} \\ &+ \sum_{\mathbf{R}\mathbf{R}'} \sigma_{\mathbf{R}} \sigma_{\mathbf{R}'} \underbrace{\int \Delta n_{loc}(\mathbf{r} - \mathbf{R}) \Delta v(\mathbf{r} - \mathbf{R}') d\mathbf{r}}_{J(\mathbf{R} - \mathbf{R}')} \\ &+ \mathcal{O}\left(\Delta v^3\right) \end{aligned}$$

$$\Delta E(\{\sigma\}) = \Delta \mu N \langle \sigma \rangle + \frac{1}{2} \sum_{\mathbf{R}\mathbf{R}'} J(\mathbf{R} - \mathbf{R}') \sigma_{\mathbf{R}} \sigma_{\mathbf{R}'} + \cdots$$

Monte Carlo Simulations

$Ga_xIn_{1-x}P$ free standing

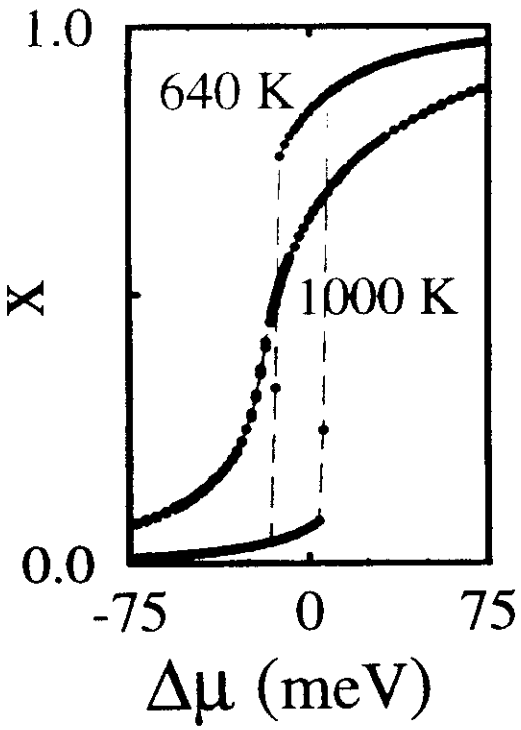

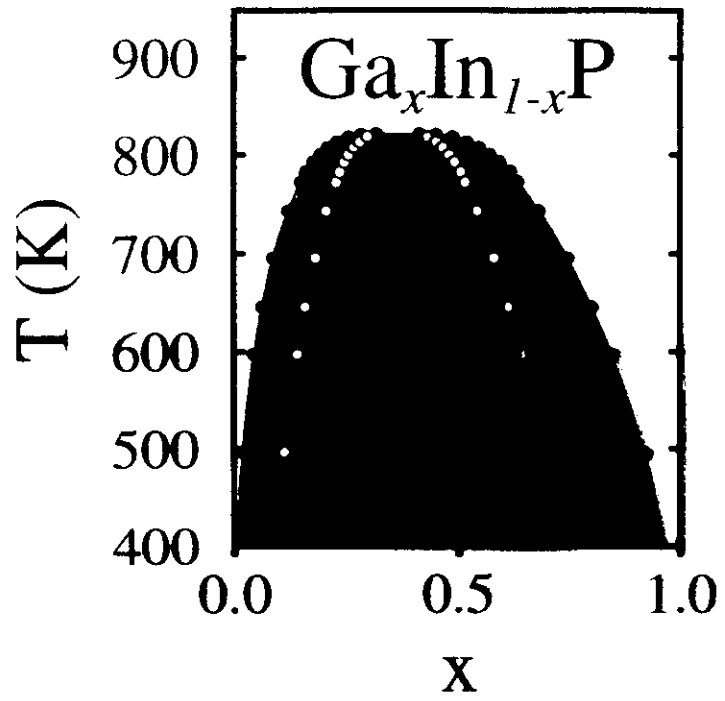

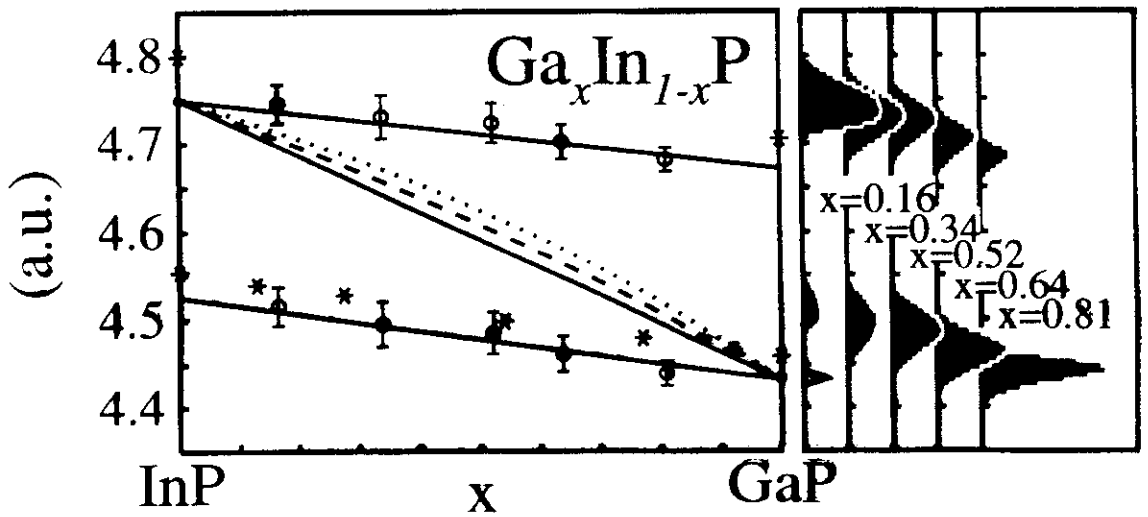

N. Marzari S. de Gironcoli S. Baroni PRL 72 4001 (1994)

Monte Carlo Simulations

$Ga_xIn_{1-x}P$ epitaxially grown on GaAs (100)

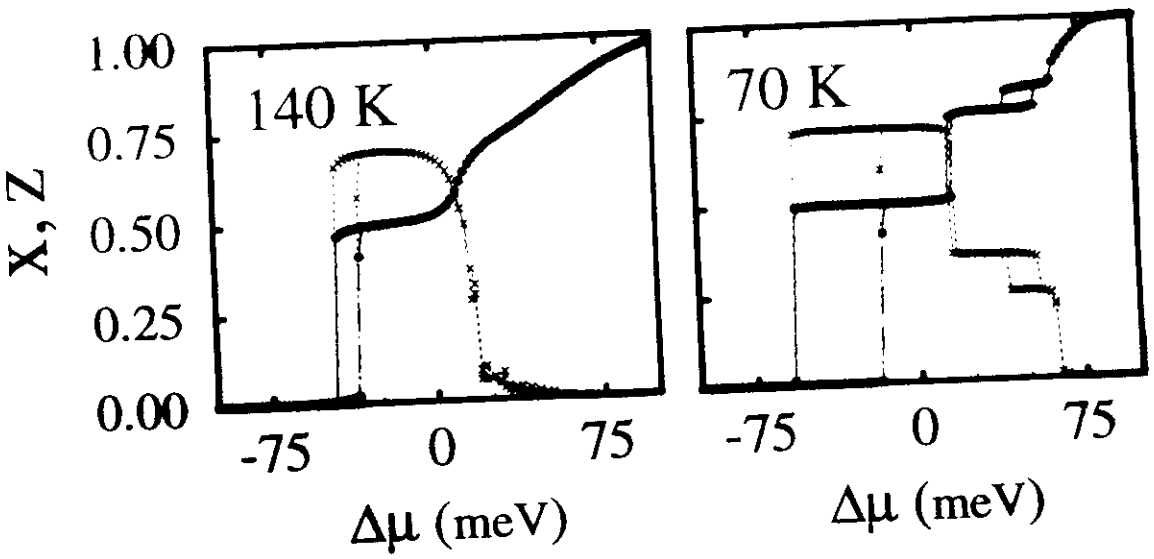

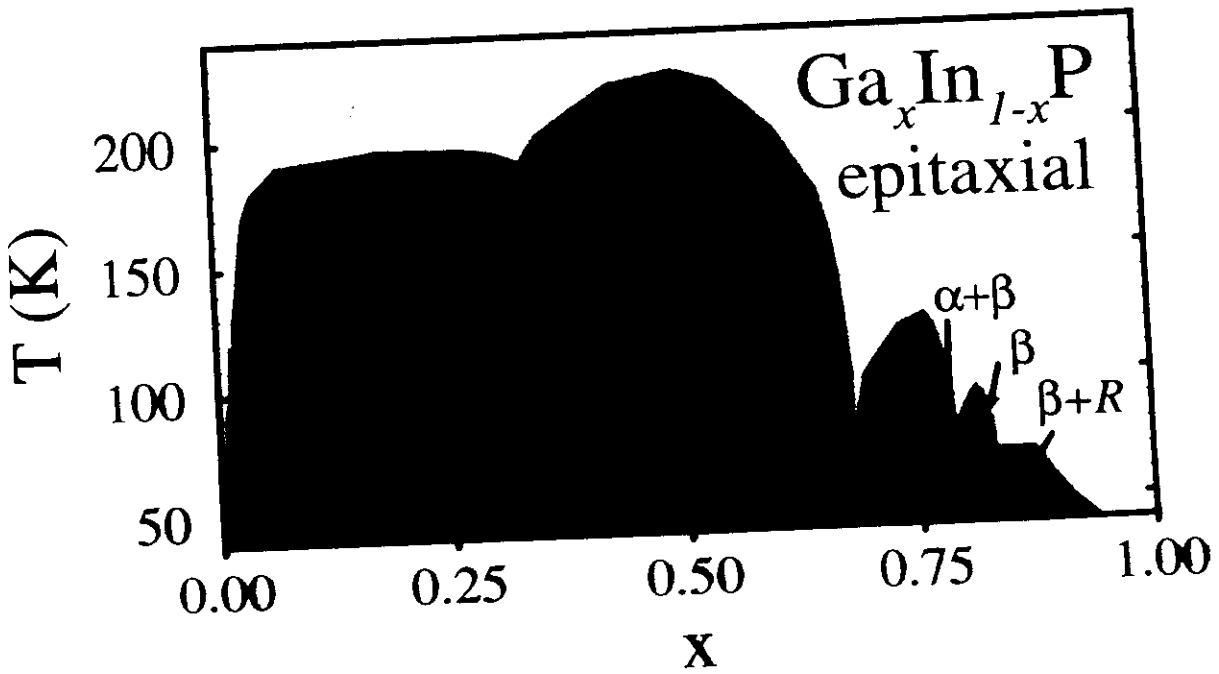

N. Marzari S. de Gironcoli S. Baroni PRL 72 4001 (1994)

Phonon dispersions of clean W(110)

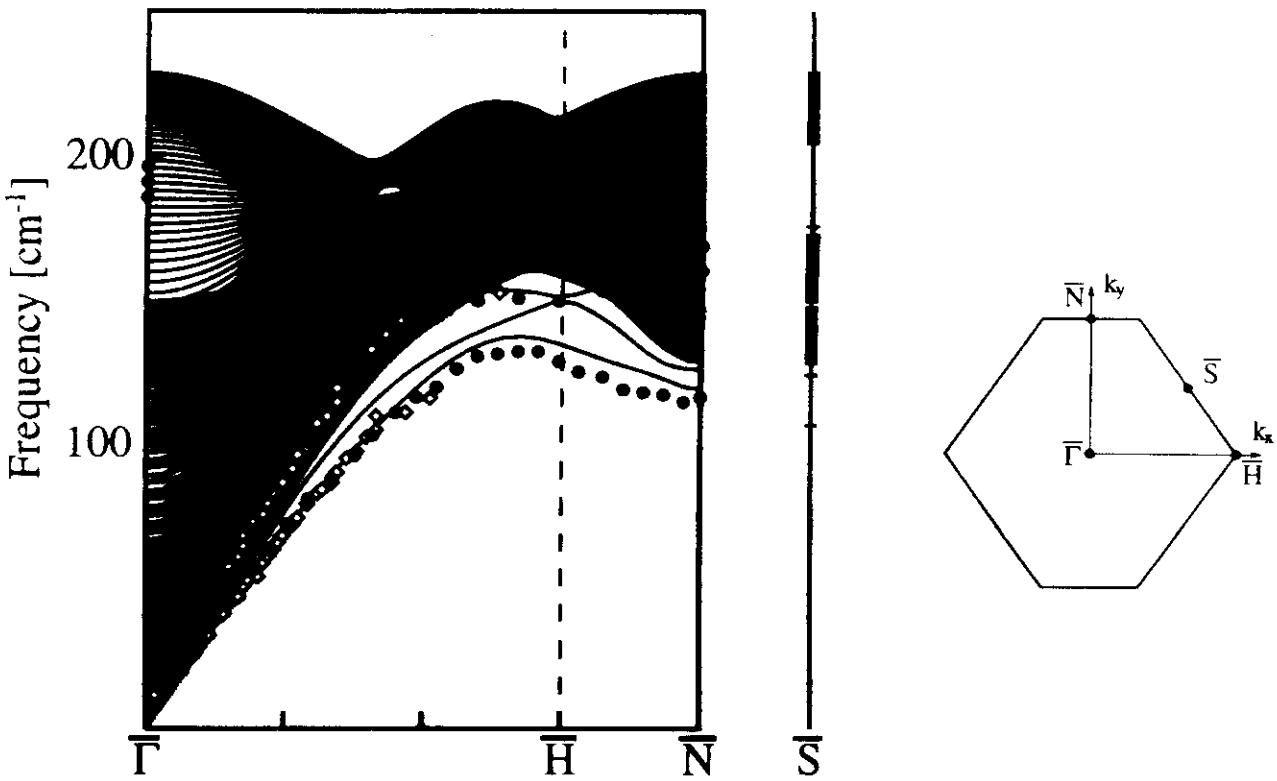

- EELS data from Balden et *al.* Surf. Sci. **307-309**, 1141 (1994).

◇ HAS data from E. Hulpke and J. Ludecke, Surf. Sci **272**, 289 (1992).

- Present calculation.
  C. Bungaro S. deGironcoli S. Baroni PRL 77 2491 (1996)

Phonon dispersions of H/W(110).

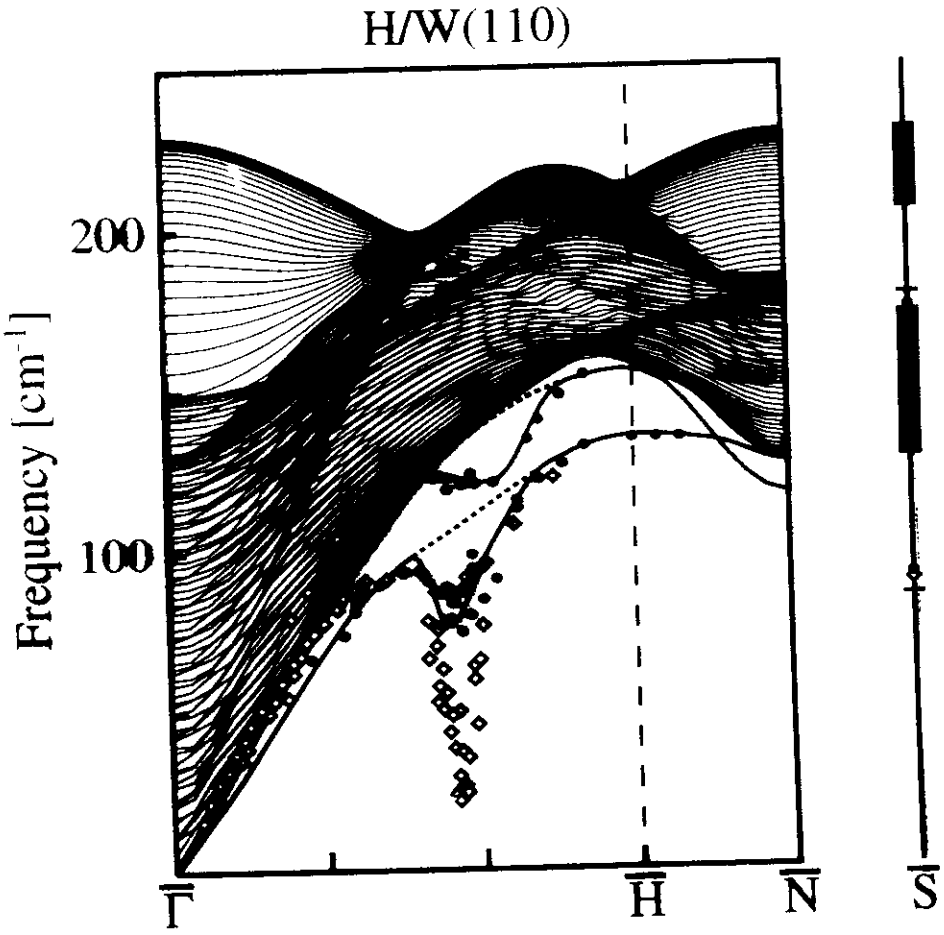

- EELS data.
- ◇ HAS data.
- Present calculation, refined results.
  C. Bungaro S. de Gironcoli S. Baroni PRL 77 2491 (1996)